

Combining two complementary micrometeorological methods to measure CH₄ and N₂O fluxes over pasture

Johannes Laubach¹, Matti Barthel^{1,2}, Anitra Fraser¹, John E. Hunt¹, and David W. T. Griffith³

[1]{Landcare Research, P.O. Box 69040, Lincoln 7640, New Zealand}

[2]{Department of Environmental Systems Science, ETH Zürich, 8092 Zürich, Switzerland}

[3]{University of Wollongong, Wollongong NSW 2522, Australia}

Correspondence to: J. Laubach (laubachj@landcareresearch.co.nz)

Abstract

New Zealand's largest industrial sector is pastoral agriculture, giving rise to a large fraction of the country's emissions of methane (CH₄) and nitrous oxide (N₂O). We designed a system to continuously measure CH₄ and N₂O fluxes at the field scale on two adjacent pastures that differed with respect to management. At the core of this system was a closed-cell Fourier-transform infrared spectrometer (FTIR), measuring the mole fractions of CH₄, N₂O and carbon dioxide (CO₂) at two heights at each site. In parallel, CO₂ fluxes were measured using eddy-covariance instrumentation. We applied two different micrometeorological ratio methods to infer the CH₄ and N₂O fluxes from their respective mole fractions and the CO₂ fluxes. The first is a variant of the flux-gradient method, where it is assumed that the turbulent diffusivities of CH₄ and N₂O equal that of CO₂. This method was reliable when the CO₂ mole-fraction difference between heights was at least 4 times greater than the FTIR's resolution of differences. For the second method, the temporal increases of mole fractions in the stable nocturnal boundary layer, which are correlated for concurrently-emitted gases, are used to infer the unknown fluxes of CH₄ and N₂O from the known flux of CO₂. This method was sensitive to "contamination" from trace gas sources other than the pasture of interest and therefore required careful filtering. With both methods combined, estimates of mean daily CH₄ and N₂O fluxes were obtained for 56 % of days at one site and 73 % at the other. Both methods indicated both sites as net sources of CH₄ and N₂O. Mean emission rates for one year

1 at the unfertilised, winter-grazed site were $8.9 (\pm 0.79) \text{ nmol CH}_4 \text{ m}^{-2} \text{ s}^{-1}$ and
2 $0.38 (\pm 0.018) \text{ nmol N}_2\text{O m}^{-2} \text{ s}^{-1}$. During the same year, mean emission rates at the irrigated,
3 fertilised and rotationally-grazed site were $8.9 (\pm 0.79) \text{ nmol CH}_4 \text{ m}^{-2} \text{ s}^{-1}$ and
4 $0.58 (\pm 0.020) \text{ nmol N}_2\text{O m}^{-2} \text{ s}^{-1}$. At this site, the N_2O emissions amounted to $1.21 (\pm 0.15) \%$
5 of the nitrogen inputs from animal excreta and fertiliser application.

6

7

8 **1 Introduction**

9 The accurate assessment of greenhouse gas (GHG) fluxes between the biosphere and the
10 atmosphere is crucial to understand driving mechanisms of global climate change. While net
11 ecosystem exchange (NEE) of carbon dioxide (CO_2) fluxes are being measured for multiple
12 years at over 400 sites around the globe, using the eddy-covariance method (Baldocchi,
13 2014), continuous methane (CH_4) and nitrous oxide (N_2O) measurements are still comparably
14 sparse at the ecosystem scale (Nicolini et al., 2013). However, the accounting of full GHG
15 budgets is especially important for agroecosystems as they are the largest global source of
16 N_2O and CH_4 emissions (Montzka et al., 2011). For instance, Leahy et al. (2004) showed that
17 N_2O and CH_4 emissions on managed grasslands have the potential to fully counteract the CO_2
18 sink strength in these ecosystems. This has been confirmed by a European wide synthesis
19 study done at 10 different grasslands sites over two years (Soussana et al., 2007). Moreover,
20 among soils from different land-use types, those from grasslands have been shown to have the
21 highest rates of N_2O emissions, due to high microbial activity stimulated by high soil C and N
22 content (Schaufler et al., 2010).

23 In order to assess effects of management and land-use changes on net GHG budgets, methods
24 are required to measure GHG fluxes at the scale at which agroecosystems are managed, which
25 is the field scale. Long-term field-scale studies of GHG fluxes in New Zealand's pastoral
26 agroecosystems are so far restricted to CO_2 only (Nieveen et al., 2005; Mudge et al., 2011).
27 Yet, 48 % of the country's total GHG emissions are CH_4 and N_2O emissions from agriculture
28 (MfE, 2015). We therefore began a project to simultaneously measure the exchange rates of
29 all three GHGs from pastures on a commercial dairy farm. In this paper, we describe and
30 critically assess our methods to measure CH_4 and N_2O fluxes and report results for these from
31 the first 20 months of this project. The reporting of CO_2 fluxes is kept brief here; for detailed
32 derivation and discussion see Hunt et al. (2016, this issue).

1 Particularly suitable for the field scale are micrometeorological methods (Denmead, 2008). Of
2 these, the eddy-covariance method has steadily increased in popularity since new types of fast
3 and precise gas analysers for CH₄ and N₂O were shown to be suitable (Eugster et al., 2007;
4 Kroon et al., 2007; Tuzson et al., 2010). In managed grasslands, eddy-covariance
5 measurements with such instruments have since been undertaken e.g. by Neftel et al. (2010),
6 Merbold et al. (2014), Hörtnagl and Wohlfahrt (2014), and Schrier-Uijl et al. (2014).

7 Disadvantages of the eddy-covariance method are that the fast analysers for CH₄ and N₂O are
8 expensive, often specific to a single gas, and frequently associated with large measurement
9 errors during periods of small fluxes (Kroon et al., 2010). Therefore, we pursue an alternative
10 approach: we use a slow, closed-cell, multi-gas analyser (FTIR spectrometer, see Section 2.1
11 for details), and we combine two other micrometeorological methods in order to maximise the
12 GHG flux information that can be gained from such measurements. One of these methods is a
13 variant of the flux-gradient method (Denmead, 2008) which we shall denote as the gas-
14 gradient ratio (GGR) method. It relies on the equality of turbulent diffusivities for different
15 gas species and is fully described in Section 2.3. The other method was first applied by
16 Kelliher et al. (2002) and will here be referred to as the nocturnal storage-ratio (NSR) method.
17 It exploits that during calm nights with stable surface-layer stratification, gases emitted at the
18 surface accumulate over time in the surface layer, much like in a natural “big chamber”. For
19 gases originating from the same locations, their mole-fraction increases in the surface layer
20 are strongly correlated, and they are easily detectable (see Section 2.4).

21 Both methods are essentially tracer-ratio methods, where we use CO₂ as the tracer, or
22 reference gas. Therefore, concurrent measurements of CO₂ fluxes are required, for which we
23 employ standard eddy-covariance instrumentation. For calm nights, we follow routine
24 practice to discard measured CO₂ fluxes (considering them unreliable) and replace them with
25 modelled values from a gap-filling algorithm. The suitability of these modelled tracer fluxes
26 for the NSR method is assessed as part of our data analysis.

27 Our choice of instruments and methods was largely guided by practical considerations.
28 Firstly, we aimed to undertake a paired-site study on two neighbouring pastures with different
29 managements. Rather than having to acquire and maintain four gas analysers, as required for
30 the eddy-covariance method with two gases at two sites (in addition to the standard CO₂-flux
31 instrumentation), it appeared a sensible alternative to employ a single multi-gas instrument
32 with a switching system, fed via long air-intake lines. Secondly, one of the two sites was

1 irrigated by a pivot irrigator that regularly passed over with a clearance height of ca. 2.5 m.
2 This constraint on measurement height made it undesirable to operate bulky open-path
3 analysers. While these conditions were very specific to our experiment, we believe that our
4 combination of methods may be useful and attractive in other measurement situations, too.

5 It is not intended here to give full greenhouse gas budgets of the dairying operations. That
6 will be the subject of future research, based on longer time series of flux measurements. In
7 particular, this study does not consider CH₄ emissions from grazing animals. We exclude all
8 periods from our analysis during which cattle were present. Following standard practice of
9 dairy farms in New Zealand, these grazing events were of only 1 to 2 d duration each, at an
10 animal density of order 100 head ha⁻¹. At this density, the fluxes of CH₄ and CO₂ would be
11 dominated by eructation and respiration, respectively, from the cattle. The cattle were then
12 moving point sources in a confined space; to measure accurate and representative fluxes from
13 these would be a challenging task, for which a number of micrometeorological methods have
14 been developed and tested elsewhere (Laubach et al., 2008; Laubach et al., 2013; Felber et al.,
15 2015). Instead, we aim to determine exchange rates of the pasture surface itself, which for
16 CH₄ are expected to be at least two magnitudes smaller than the emission rates from a grazing
17 cattle herd.

18 The first objectives of this paper are to describe the GGR and NSR method in detail and to
19 identify for each the conditions in which it reliably operates (or otherwise). Based on that
20 assessment, we aim to specify data-filtering criteria for each method. We then compare results
21 between the two methods and assess how they should be combined to obtain reliable annual
22 mean fluxes of CH₄ and N₂O from the pasture surfaces. In the case of the irrigated pasture, we
23 are able to relate the measured N₂O fluxes to the nitrogen (N) inputs from fertilisation and
24 excreta deposition.

25

26

27 **2 Materials and methods**

28 **2.1 Site and farming operations**

29 The study was conducted on an intensively managed dairy farm (ca. 900 cows on 382 ha) on
30 the Canterbury Plains, South Island, New Zealand (Lat -43° 35' 30.6", Lon 171° 55' 36.6");

1 204 m a.s.l.). The soil is a Lismore silty loam which is moderately stony and well-drained.
2 The farm was converted to irrigated dairying in 2008. The irrigated pasture is dominated by
3 ryegrass (*Lolium perenne* L.) with a minor fraction of white clover (*Trifolium repens* L.). The
4 main irrigated area (263 ha) is circular and subdivided into 19 similar-sized paddocks. Part of
5 the farm is an area of non-irrigated land, wedged between this farm's irrigated circle to the S
6 and a similar irrigated circle of the neighbouring farm to the W (Fig. 1). We established two
7 measurement sites in mid-2012, one inside the irrigated circle at ca. 140 m distance from the
8 perimeter, the other inside the dryland wedge, at a similar distance from its boundaries to S
9 and W. Instrumentation connected to both sites was operated in a hut placed at the boundary
10 between the irrigated and the dryland pasture (Fig. 1).

11 The farm managers monitored volumetric water content (VWC) of the pasture soil (10 to
12 40 cm depth) and used the pivot irrigator to keep VWC above $0.2 \text{ m}^3 \text{ m}^{-3}$. The irrigated
13 pasture was fertilised 9 times annually, on the majority of occasions with urea; in the 2012/13
14 season, the total application rate was $18.3 \text{ g N m}^{-2} \text{ yr}^{-1}$. Throughout the milking season
15 (September to late April) each paddock was grazed 8 to 12 times, usually by 400 to 500 cows.
16 For our measurement site, times of grazing events were recorded. Effluent collected at the
17 milking shed was recycled to the pasture via irrigator attachments. We will refer to our
18 measurement site on the irrigated, fertilised, rotationally-grazed pasture as the "IFR site"; for
19 future reference in the Fluxnet network it has been named "NZ-BFm" (D. Papale, pers.
20 comm., 2016).

21 The dryland pasture was used for winter-grazing once in July 2012, prior to the start of our
22 measurements, and once in May 2013, otherwise it was not managed during the 2012/13
23 season. The measurement site there is labelled as the "UW site" (unirrigated, unfertilised,
24 winter-grazed); its future Fluxnet name will be "NZ-BFu". On 28 October 2013 the pasture
25 was sprayed with herbicide, followed by sowing kale (*Brassica oleracea* L., cultivar "corka")
26 on 20 November, to provide a forage crop for winter 2014.

27

1 2.2 Instrumentation

2 2.2.1 Mole fraction measurements of CH₄, N₂O and CO₂

3 Mole fractions of the trace gases CO₂, CH₄, N₂O and CO were measured simultaneously with
4 a Fourier-transform infrared (FTIR) trace gas analyser built at the University of Wollongong
5 (Griffith et al., 2012). The analyser is equivalent to the now commercially available
6 Spectronus analyser (Ecotech, Knoxfield, VIC, Australia). This instrument performs
7 broadband-spectrum absorption measurements and uses an optimisation algorithm called
8 MALT to retrieve mole fractions of the trace gas species of interest from the measured
9 infrared spectra. For details of both the FTIR hardware and the MALT algorithm see Griffith
10 et al. (2012).

11 The FTIR was housed in the hut midway between the two measurement sites. From two
12 heights ($z_1 = 0.76$ m, $z_2 = 1.96$ m), at each site, air was drawn continuously via 170 m long
13 nylon tubing, buried at 0.2 m depth, into 10 L stainless steel cylinders (ballast tanks) inside
14 the hut. A fifth air intake was at 10 m height, next to the hut, to sample gas mole fractions
15 representative of the wider surroundings. All five air streams were drawn in parallel with a
16 dual-head diaphragm pump (2107AC, Gardner Denver Thomas, Sheboygan, Wisconsin,
17 USA). The FTIR was operated in discrete cell-fill mode, sampling air from each of the five
18 ballast tanks once over the course of a 30-min cycle. During every 29th cycle, the
19 measurement from 10 m was skipped, and instead a sample was taken from a cylinder
20 containing air with known mole fractions of the gases of interest (“target tank”), to check for
21 calibration drifts. An external manifold unit with solenoid valves switched between the
22 different sample and calibration intakes. A four-diaphragm oil-free vacuum pump (MV 2 NT,
23 Vacuubrand, Wertheim, Germany) served to evacuate the FTIR’s measurement cell to about
24 2.5 hPa and then to refill it with sample air. Before entering the cell, the sample air was dried
25 in two stages, with a Nafion[®] drier and a magnesium perchlorate trap. This resulted in water
26 vapour mole fractions $< 10 \mu\text{mol mol}^{-1}$, which were included in the mole fractions retrieved
27 by the MALT algorithm.

28 The FTIR was run in static mode according to the following measurement cycle procedure:
29 1) cell and manifold evacuation for 120 s, reaching ca. 3 hPa; 2) cell fill to 900 hPa (for up to
30 a maximum duration of 120 s); 3) cell pressure stabilisation for 60 s, 4) spectrum collection
31 and analysis for 60 s, then wait to the end of 6 min and repetition of these steps for the next

1 intake line. Because the previous sample was not completely removed from the cell, the
2 measured mole fractions were corrected for the residual sample in the cell from the previous
3 measurement. Since $[\text{N}_2\text{O}]$ and $[\text{CH}_4]$ differences between intakes were often less than the
4 resolution limits (see Results section), we tested whether the measurement precision could be
5 improved by allowing more time for Step 4). This was found to be the case, therefore in a new
6 measurement cycle, the time for Step 4) was increased 7-fold, allowing far more individual
7 spectra to be collected and analysed for each cell fill. As the new cycle required 60 min total
8 duration for the five intakes, intakes at only one site could be sampled each half-hour.
9 Therefore, the increased precision came at the cost of halving the data yield. With more time
10 per intake available, the cell-fill pressure was increased to 950 hPa (to achieve a further
11 modest gain in precision) and up to 140 s were allowed for the filling process (Step 2). The
12 new cycle was used from 15 October 2013 onwards.

13 The hut temperature was controlled at $20 (\pm 2) ^\circ\text{C}$, and the measurement cell of the FTIR was
14 thermostat-regulated to $30 ^\circ\text{C}$. Cell temperature during measurements was recorded and used
15 in the retrieval of gas mole fractions from the spectra (Griffith et al., 2012). The cell
16 temperature was found to respond to changes in hut temperature at a rate of 0.01 K K^{-1} .

17 The FTIR was calibrated with three different gas cylinders of clean southern-hemisphere
18 background air, spiked with varying mole fractions for each species of interest. These
19 cylinders had been filled and their contents composition measured by the National Institute of
20 Water & Atmospheric Research (Wellington, New Zealand), following the standards of the
21 WMO's Global Atmospheric Watch programme. Calibrations were carried out 8 times over a
22 20-month period and yielded very consistent results: the calibration slopes (of measured vs
23 nominal mole fractions) showed no systematic variation over time, and their relative standard
24 deviations were 0.14 % for CO_2 , 0.08 % for CH_4 , and 0.16 % for N_2O .

25

26 2.2.2 CO_2 flux measurements and gap-filling

27 At each site, an eddy covariance (EC) system was operated to measure the fluxes of CO_2 ,
28 water vapour, heat and momentum at 1.86 m above ground. The system consisted of an
29 enclosed infrared gas analyser to measure CO_2 and H_2O vapour concentrations (LI-7200, LI-
30 COR Biosciences, Lincoln, NE, USA) and an ultrasonic anemometer to measure the wind
31 vector and temperature (WindMaster Pro, Gill Instruments, Lymington, Hampshire, UK). The

1 raw 20 Hz time series were collected with an Analyzer Interface Unit (LI-7550, LI-COR
2 Biosciences, Lincoln, NE, USA). Data corrections, averaging and flux computation were
3 performed with the open-source software EddyPro (LI-COR Biosciences, Lincoln, NE, USA).
4 Further details of the EC setup are given in Hunt et al. (2016, this issue).

5 The CO₂ flux data were filtered to exclude grazing periods, periods of instationary wind
6 conditions, and periods of low turbulence. The last were flagged by $\sigma_w = 0.12 \text{ m s}^{-1}$, where σ_w
7 is the standard deviation of vertical wind speed, following Acevedo et al. (2009) who argue
8 this is a more selective filter than the commonly-used friction velocity threshold. The ensuing
9 data gaps were filled with an artificial-neural-network method, known as the SOLO (self-
10 organizing linear output) model (Hsu et al., 2002), which has been shown to be accurate on a
11 daily basis (Eamus et al., 2013).

12 At the IFR site, small-scale CO₂ flux measurements with four automated respiration chambers
13 (LI-8100A, LI-COR Biosciences, Lincoln, NE, USA) were available for part of the
14 measurement period. These chambers were placed ca. 3 m from the EC mast, within a fenced
15 area from which the cows were excluded. They received the same irrigation and fertilisation
16 applications as the surrounding paddock. The grass inside the chambers was cut manually
17 when the surrounding paddock was grazed, and on these occasions, urea was hand-applied to
18 simulate the additional N input from excreta deposited by grazing animals. Data from these
19 chambers are used to corroborate the nocturnal CO₂ fluxes obtained from EC measurements
20 and SOLO gap-filling.

21

22 2.2.3 Ancillary measurements

23 Alongside the EC measurements, each site was equipped to record half-hourly averages of
24 precipitation, radiation, wind speed and direction, PAR, relative humidity, air temperature,
25 soil heat flux and direct and diffuse radiation. Also, soil temperature and soil VWC were
26 recorded in three separate profiles per site, at depths of 5, 10, 25, and 50 cm. Soil temperature
27 was measured with copper/constantan thermocouples and VWC with time-domain
28 reflectometry probes (SM300, Delta-T Devices, Burwell, Cambridge, UK).

29

1 2.3 Gas-gradient ratio method

2 The gas-gradient ratio (GGR) method is a variant of what is commonly known as the flux-
3 gradient method. In the latter, the flux F_χ of a gas species χ is computed as the product of the
4 (negative) vertical concentration gradient with a turbulent diffusivity. In practice, the
5 infinitesimal gradient is approximated by finite differences, which gives:

$$6 \quad F_\chi = -K_\chi C_{\text{air}} \frac{[\chi]_1 - [\chi]_2}{z_1 - z_2} \quad (1)$$

7 where $[\chi]$ is the mole fraction and K_χ the turbulent diffusivity of χ , C_{air} the molar density of
8 dry air, z height above ground, and the subscripts 1 and 2 indicate measurement heights.
9 Upward fluxes (away from the surface) are represented with positive values, following the
10 micrometeorological convention. The diffusivity is parameterised using similarity theory
11 (Oke, 1987; Denmead, 2008). Often, the parameterisation is based on momentum exchange;
12 this approach is also known as the aerodynamic method (Oke, 1987; Denmead, 2008). There,
13 the diffusivity of momentum, K_m , is usually specified as:

$$14 \quad K_m = k u_* z \phi^{-1} \quad (2)$$

15 where k is the von-Kármán constant, u_* friction velocity, and ϕ a function of stratification. To
16 make use of (2), the ratio of the diffusivities for momentum and mass, K_m/K_χ (named the
17 turbulent Schmidt number) must be known; yet, how this number varies with height scale and
18 flow statistics in the surface layer is difficult to measure and different approaches have
19 yielded contradictory results (Wilson, 2013). By contrast, there is less ambiguity about the
20 relationships between the diffusivities of different scalar variables, such as heat, moisture and
21 trace gas concentrations. For a pair of scalars with similar spatial distribution of their
22 source/sink locations, the diffusivities are equal, except for small differences between heat
23 and gases with regard to effects of thermal stratification. Thus, by measuring the flux and the
24 gradient of a reference scalar variable, the diffusivity can be obtained. For example, Phillips et
25 al. (2007) used heat as the reference variable to derive N_2O fluxes over pasture, and Griffith et
26 al. (2002) used water vapour as the reference to obtain fluxes of CO_2 , CH_4 and N_2O . In both
27 cases, this method was largely restricted to daytime (because fluxes and gradients of heat and
28 water vapour are small at night). Here, we use CO_2 as the reference variable, a choice
29 successfully employed to measure CH_4 emissions from rice crops (Miyata et al., 2000,
30 McMillan et al., 2007). From Eq. (1), its turbulent diffusivity is given by:

$$1 \quad K_{\text{CO}_2} = -\frac{F_{\text{CO}_2}}{C_{\text{air}} \Delta[\text{CO}_2]} \Delta z \quad (3)$$

2 where Δ indicates the difference between heights, i.e. $\Delta[\text{CO}_2] = [\text{CO}_2]_1 - [\text{CO}_2]_2$ and
 3 $\Delta z = z_1 - z_2$. Assuming $K_\chi = K_{\text{CO}_2}$ where χ now refers to the non- CO_2 gas species, and
 4 inserting Eq. (3) back into Eq. (1) results in:

$$5 \quad F_\chi = \frac{\Delta[\chi]}{\Delta[\text{CO}_2]} F_{\text{CO}_2} \quad (4)$$

6 The gas-gradient ratio, $\Delta[\chi]/\Delta[\text{CO}_2]$, is independent of flow properties, such as wind speed
 7 or stratification.

8 Since fluxes and gradients of CO_2 undergo sign changes in the morning and evening, periods
 9 including these transitions will need to be excluded. It is expected that these periods of near-
 10 zero $[\text{CO}_2]$ gradients often coincide with periods that are unsuitable for the GGR method
 11 anyway, because the surface-layer undergoes transitions between unstable and stable
 12 stratification and flow conditions will not be steady enough to define a meaningful diffusivity.

13

14 **2.4 Nocturnal storage-ratio method**

15 During clear night-time periods, cooling of the ground surface due to long-wave radiation
 16 losses causes stable stratification of the atmospheric surface layer. In this nocturnal inversion
 17 layer, turbulent exchange is suppressed and wind speeds are low. Consequently, trace gases
 18 emitted from the ground, or the biosphere near the ground, accumulate in this layer over time.
 19 This accumulation process underlies the principle of the nocturnal storage-ratio (NSR)
 20 method. Provided that the spatial distribution and temporal pattern of emissions are similar for
 21 different gas species, their mole-fraction increases over time must be strongly correlated with
 22 each other. This is illustrated in Fig. 2, where changes in $[\text{CH}_4]$, $[\text{CO}_2]$ and $[\text{N}_2\text{O}]$ track each
 23 other well: the mole fractions increase sharply when σ_w falls below 0.12 m s^{-1} , and they return
 24 towards their baseline values when σ_w rises persistently above 0.12 m s^{-1} . The correlations
 25 between the mole fractions of the trace gases are exploited to link the unknown flux of a gas
 26 species χ with the known flux of another gas, here CO_2 , as follows (Kelliher et al., 2002;
 27 Pendall et al., 2010). The relationship between the mole-fraction increases, $d[\chi]$ and $d[\text{CO}_2]$,

1 is assumed linear and expressed by the slope of a linear regression. The flux of χ is then
2 computed as the product of the CO₂ flux with the regression slope:

$$3 \quad \overline{F_{\chi}} = \frac{\overline{d[\chi]}}{\overline{d[\text{CO}_2]}} \overline{F_{\text{CO}_2}} \quad (5)$$

4 where the overbars indicate whole-night averages. This method is only applied for sufficiently
5 calm nights, and the regression slope determined separately for each of these.

6 During calm conditions, flux measurements by eddy covariance are notoriously unreliable.
7 Kelliher et al. (2002) and Pendall et al. (2010) used respiration chambers to measure the CO₂
8 flux instead. Here, we try a different approach. We define calm conditions by the same low-
9 turbulence threshold that is used to filter the CO₂ fluxes measured by eddy covariance prior to
10 gap-filling, as illustrated in Fig. 2. We then use the CO₂ fluxes constructed by the gap-filling
11 algorithm as inputs for the NSR method. Since Eq. (2) applies to whole nights, it is not the
12 accuracy of the half-hourly gap-filled fluxes that matters, but only the accuracy of their
13 whole-night average. We will assess the suitability of gap-filled CO₂ fluxes for deriving other
14 trace gas fluxes with the NSR method (Section 3.3.2).

15

16 **2.5 Measurement period**

17 We analyse measurements from the period 17 August 2012 to 31 March 2014, including one
18 full grazing/irrigation season, the larger fraction of a second one, and the winter between
19 these. The FTIR operated continuously, except for short maintenance and calibration periods
20 (a few hours each) and one fortnight of mains-power outage (10 to 24 September 2013)
21 following widespread windstorm damage in the region. Data collected during grazing events
22 were excluded because the CO₂ and CH₄ gradients were dominated by emissions from the
23 animals, which vary erratically with animal positions, and fluxes originating at the pasture
24 surface cannot be retrieved. At the IFR site, grazing events usually lasted only 1 to 2 d; at the
25 U UW site, there were only two grazing periods, in May 2013 and in late October 2013 (just
26 prior to the conversion to kale). The grazing dates of other irrigated paddocks, outside the one
27 containing our measurement site, were not recorded. Data filtering criteria for the GGR and
28 NSR method are explored in the Results section.

1

2

3 **3 Results**

4 **3.1 Soil and vegetation conditions, and CO₂ fluxes**

5 Soil temperatures at 5 cm depth ranged from 2.5 °C to 22.3 °C at the IFR site and from 1.5 °C
6 to 23.5 °C at the UUW site, with the minima occurring in early July and the maxima in late
7 January. Rainfall in the year starting 17 August 2012 was 1014 mm, of which 407 mm fell in
8 the warmer half (October – March). At the IFR site, this was supplemented with 425 mm of
9 irrigation to keep the pasture well-watered throughout the grazing season. The irrigator
10 rotated continuously from mid-spring (October) to mid-autumn (early April), with a return
11 period of about 3 d, applying about 10 L m⁻². As a result, soil VWC at 5 cm depth stayed
12 above 0.24 m³ m⁻³. Meanwhile, the UUW site experienced drought conditions from mid-
13 December 2012 until mid-March 2013, with VWC in the range 0.06 to 0.15 m³ m⁻³.

14 Over the remaining 7.5 months (after 16 August 2013), 598 mm of natural precipitation
15 occurred. In this period, the start of the irrigation was delayed until mid-November 2013, due
16 to storm damage to the irrigator. When irrigation began, VWC at 5 cm had already fallen to
17 ca. 0.15 m³ m⁻³, at both sites. This irrigation season was terminated on 19 Feb 2014 with the
18 onset of sufficient natural rainfall; the total irrigation in 2013/14 amounted to 345 mm.

19 Fig. 3 shows the time courses of daily mean CO₂ fluxes (net ecosystem exchange), computed
20 from gap-filled half-hourly fluxes, excluding days on which grazing occurred. At the IFR site,
21 each grazing event turned the pasture abruptly from a CO₂ sink (negative mean flux) to a CO₂
22 source (positive mean flux), while the leaf area index was reduced from 2.7 to 0.6 m² m⁻²
23 (Hunt et al., 2016). After a few days of regrowth, the flux reversed sign and the CO₂ sink
24 strength increased steadily, until the next grazing. As a consequence of the regular
25 fertilisation and irrigation, the pasture was highly productive.

26 The UUW site, by contrast, acted as a CO₂ sink mainly in the two spring seasons (Sept to
27 Nov) and during the growth of the kale crop in the 2013/14 summer. A prominent feature in
28 Fig. 3 is the change from sink to source in December 2012 as a consequence of the drought
29 conditions. From then until the next spring, the UUW pasture remained a weak CO₂ source.

1 Also clearly visible in Fig. 3 is the disturbing effect of the conversion to kale, making the site
2 temporarily a stronger CO₂ source in Nov-Dec 2013, until the kale crop had established itself.
3

4 **3.2 GGR method**

5 3.2.1 Mole-fraction gradients and instrument precision

6 The short-term repeatability of the FTIR's mole-fraction measurements was determined by
7 repeatedly filling the cell with target-tank air and otherwise following the same switching-
8 cycle sequence as described in Section 2.2.1. With the original cycle (total time of 6 min per
9 intake), the standard deviation (SD) of the target-tank [N₂O] was 0.28 ppb; with the modified
10 cycle (12 min per intake), this was halved to 0.14 ppb (Table 1). For [CH₄], the SD of the
11 same target-tank samples was 0.58 ppb with the original cycle and reduced to 0.20 ppb with
12 the modified cycle. For [CO₂], the effect of the change in cycle was less pronounced, with an
13 SD of 0.15 ppm with the original cycle and 0.12 ppm with the modified cycle.

14 In Table 1, the mean mole fractions using the original cycle and the modified cycle tend to
15 differ by more than the observed SD values (particularly strongly for CH₄). The likely cause
16 of this is that with the original cycle the spectral measurements were made before the cell
17 contents had thermally equilibrated. While this lack of equilibrium causes small biases in the
18 mole fractions, the repeatability of these is not affected (as attested by the observed SD
19 values), and mole-fraction differences between intakes (GGR method) or between successive
20 nighttime hours (NSR method) are unbiased.

21 To define a „precision“, the acceptable probability of a single measurement deviating
22 randomly by more than this precision from the mean value must be specified. If we take the
23 acceptable probability as 5 %, then the precision is given as 3 times the SD of repeated
24 sampling. The resolution of a gradient measurement (mole-fraction difference between two
25 intakes) follows directly as 2^{1/2} times that precision: differences smaller than that cannot be
26 considered significantly different from zero. Such non-resolvable mole-fraction differences
27 between intakes occurred frequently, for all three gases. According to Eq. (3), a non-
28 resolvable gradient of gas species χ (N₂O or CH₄) simply implies a non-resolvable flux of that
29 species, in proportion. When many repeated measurements are made over time to determine a
30 mean flux, those runs with non-resolvable fluxes still make valid contributions: as the

1 standard error of the mean (SEM) decreases with increasing number of samples, the sign (and
2 magnitude) of the mean flux becomes better-resolved. Hence, small gradients of [N₂O] or
3 [CH₄] were not removed from the dataset.

4 By contrast, $\Delta[\text{CO}_2]$ appears in the denominator of Eq. (3), with the consequence that small
5 values of it lead to highly uncertain fluxes of χ . Thus, the data must be filtered for a minimum
6 $\Delta[\text{CO}_2]$. We test this by its effect on the diffusivity, as follows.

7

8 3.2.2 Turbulent diffusivities

9 Half-hourly values for the gas diffusivity, K_{CO_2} , computed with (3), are compared in Fig. 4
10 against the momentum diffusivity, K_m , for neutral stratification, i.e. using (2) with $\phi = 1$.
11 These data are shown both for all available runs and for two selections with a minimum
12 $\Delta[\text{CO}_2]$, of 0.6 ppm and 2.4 ppm (ca. 1 and 4 times the resolution of the FTIR for CO₂). The
13 unfiltered gas diffusivity data are widely scattered, even outside the margins of the figure. The
14 smaller $\Delta[\text{CO}_2]$ threshold constrains the K_{CO_2} values, by and large, to the range -0.6 to
15 $1 \text{ m}^2 \text{ s}^{-1}$, proving that a large part of the scatter originates from small values in the
16 denominator of (3) subject to large relative errors. The larger $\Delta[\text{CO}_2]$ threshold reduces the
17 K_{CO_2} range further, to about -0.1 to $0.4 \text{ m}^2 \text{ s}^{-1}$. The positive side of this range is similar to the
18 range of momentum diffusivities and therefore considered realistic. The negative side is due
19 to sign mismatches between CO₂ fluxes and gradients. Most of these occur around the
20 morning and evening transitions, indicating that at such times the surface fluxes and surface-
21 layer gradients are not in equilibrium, and that the application of a simple flux-gradient
22 concept is then not appropriate. All runs with negative K_{CO_2} are thus excluded from further
23 analysis, in addition to the runs with $\Delta[\text{CO}_2] < 2.4$ ppm.

24 Turbulent diffusivities are positively correlated with wind speed; for K_m this is evident from
25 the dependence on u_* in (2). In Fig. 4, it is apparent that filtering with the larger $\Delta[\text{CO}_2]$
26 threshold removes almost all values measured at higher wind speeds. The higher the wind
27 speed, the better the turbulent mixing, and consequently, the smaller the vertical gradients of
28 any scalar variables. As these gradients approach their resolution limits, the GGR method
29 becomes inaccurate. Here, a minimum threshold for $\Delta[\text{CO}_2]$ of 2.4 ppm implies a maximum
30 wind speed of approximately 5 m s^{-1} .

1

2 3.2.3 Filter thresholds and data yield

3 Of over 22,000 runs with measured $\Delta[\text{CO}_2]$, 9193 for the IFR site and 6912 for the UUW site
4 passed the $\Delta[\text{CO}_2]$ threshold value. The higher rejection rate for the UUW site is consistent
5 with CO_2 fluxes and gradients at that site being generally closer to zero than at the IFR site. A
6 few hundred runs were eliminated during grazing events. Further, since the CO_2 fluxes for
7 runs with $\sigma_w < 0.12 \text{ m s}^{-1}$ were excluded and replaced with gap-filled values, such runs were
8 not used for the GGR method. Of the remaining runs, 6 % at the IFR and 13 % at the UUW
9 site had to be discarded because of negative K_{CO_2} , leaving 3757 and 2424 runs, respectively.
10 The overall relative data yield of the GGR method was thus 17 % at the IFR site and 11 % at
11 the UUW site.

12

13 3.2.4 Footprint considerations

14 For the CO_2 fluxes measured by eddy covariance, the footprints were computed with the tool
15 of Neftel et al. (2008), which implements the model of Kormann and Meixner (2001). The
16 footprint contributions from the target surface were found $> 90 \%$ most of the time, at both
17 sites (Hunt et al., 2016).

18 Flux footprints depend on measurement height. For the trace gas fluxes using the GGR
19 method, the effective measurement height must be somewhere between the heights of the two
20 intakes (0.76 and 1.96 m). This intermediate height, regardless of how exactly it is specified,
21 is lower than the eddy-covariance measurement height (1.86 m), hence the footprint
22 contributions of the target surface to the CH_4 and N_2O fluxes are even larger than for the eddy
23 fluxes. Compared to the overall uncertainty of the fluxes, the footprint contributions from
24 areas outside the target surface are thus considered negligible, and no wind-direction filtering
25 was applied to the data.

26

27 3.2.5 Diurnal courses and daily means of fluxes

28 An example of CH_4 and N_2O fluxes obtained with the GGR method is shown in Fig. 5, along
29 with wind speed. Some negative flux values occur, and since negative diffusivities have been

1 explicitly excluded, these must be due to positive (upwards-increasing) gradients. Data yield
2 is higher at the IFR site, as already noted to be the case throughout. At both sites the range of
3 N₂O fluxes is fairly consistent from one day to the next, the daily mean N₂O fluxes are
4 positive for all days shown, and the scatter is of the same magnitude as the mean. For the CH₄
5 fluxes, the picture is less consistent: on some days (e.g. 14 Feb) the range is much larger than
6 on others (e.g. 17 Feb), the large range includes positive and negative fluxes, and on days
7 with such a large range the scatter is much larger than the mean and makes the latter's value
8 highly uncertain. The days with large scatter tend to be windier than those without, so in part
9 the large scatter may be due to relatively small CH₄ gradients, near the FTIR resolution limit,
10 being multiplied with large diffusivities, which in effect amplifies the random error of the
11 gradient measurements. This can of course occur for N₂O, too. Another possibility, more
12 specific to CH₄, is the existence of large sources, such as grazing animals, in nearby
13 paddocks. Temporal variations of wind direction may cause the emissions plumes from such
14 sources to contaminate the air sampled from either intake. Since the intakes are sampled
15 sequentially, the sign and magnitude of the contamination effect on the gradient would then
16 depend strongly on the exact timing of such a plume's passage. Lacking detailed information
17 of cattle presence in paddocks other than the target paddocks, we do not have any objective
18 criteria to decide which CH₄ flux records are contaminated. Hence, we only apply a crude
19 outlier filter, by removing fluxes that fall outside ± 5 times the SD of the whole dataset.

20 Assuming that no strong diurnal courses are expected for either CH₄ or N₂O fluxes, and that
21 the within-day variability of both is largely random, we assess seasonal variability from daily
22 means and their standard errors (SE). Days with fewer than four valid runs were excluded.
23 Daily fluxes were obtained on 59 % and 38 % of all days for the IFR and the UUW site,
24 respectively. These were spread reasonably evenly across all seasons (Figs. 6, 7), with the
25 lowest coverage in June (early winter).

26 At both sites, daily means of CH₄ fluxes using the GGR method were generally small
27 compared to their SE and thus often not significantly different from zero. No seasonal trends
28 were discernible, and no quasiperiodic patterns that could be associated with the rotational
29 grazing, either. The median daily CH₄ fluxes were 3.7 and 4.9 nmol m⁻² s⁻¹ at the IFR and the
30 UUW site, respectively, indicating small net emissions overall; the median SE of these daily
31 fluxes were 8.2 and 7.8 nmol m⁻² s⁻¹, respectively.

1 Daily means of N₂O fluxes from the GGR method also occurred with either sign (middle
2 panels of Figs. 6, 7); however, after 15 October 2013, when the modified switching cycle
3 (12 min per intake) was used, negative daily fluxes became rare. At the IFR site, daily N₂O
4 fluxes spanned the range $\pm 5 \text{ nmol m}^{-2} \text{ s}^{-1}$, but the majority of values were of positive sign.
5 The median daily flux was $0.52 \text{ nmol m}^{-2} \text{ s}^{-1}$. This was greater than the median of the
6 associated SE values, of $0.39 \text{ nmol m}^{-2} \text{ s}^{-1}$, and thus indicated significant net emissions
7 overall. At the U UW site, daily N₂O fluxes ranged from -1.2 to $1.9 \text{ nmol m}^{-2} \text{ s}^{-1}$. The median
8 flux was $0.28 \text{ nmol m}^{-2} \text{ s}^{-1}$, and the median SE of the daily fluxes was $0.29 \text{ nmol m}^{-2} \text{ s}^{-1}$,
9 respectively. As with CH₄, it was difficult to detect any seasonal trends, except for a slight
10 tendency for larger variability throughout the irrigation seasons (which are largely identical
11 with the seasons of N inputs from grazing and fertiliser application). In particular, there were
12 no obvious responses of N₂O fluxes to soil moisture (bottom panels of Figs. 6, 7).

13

14 3.3 NSR method

15 3.3.1 NSR regressions

16 For the NSR method, linear regression slopes for N₂O and CH₄ mole fractions versus CO₂
17 mole fraction were determined for each night in which runs with $\sigma_w < 0.12 \text{ m s}^{-1}$ occurred
18 (including only these runs in the regression). To be reliable, the linear relationship must have
19 a high R² and must be based on a sufficient number of runs, n . Therefore, minimum
20 thresholds for both parameters are required. During most low-turbulence nights, the
21 regressions of [N₂O] versus [CO₂] had R² values greater than 0.7, at both sites. There was no
22 relationship between R² and n , except that the scatter in R² seemed to increase with
23 decreasing n (not shown). For [CH₄], the R² values of the NSR regressions versus [CO₂]
24 tended to be lower than for [N₂O]; their majority spread between 0.3 and 0.8, again
25 irrespective of n . Lacking any obvious cut-off values for R² and n , their choices must be made
26 pragmatically by balancing the reliability of the individual regression (in favour of high
27 thresholds) against the statistical power of including a large number of nights (in favour of
28 low thresholds). We used a minimum R² = 0.4 and a minimum $n = 4$, which leaves about
29 29 % of nights available for CH₄ and about 48 % for N₂O.

30 Fig. 8 shows the evolution of the NSR regression slopes over time. For three quarters of the
31 year, the N₂O vs CO₂ slopes show mainly short-term variations, but hardly any seasonal

1 trend; yet during the colder months May to July they increase to 3 to 5 times higher levels.
2 Both the short-term and the seasonal variations are very similar for the two sites. The CH₄ vs
3 CO₂ slopes are less well correlated between the two sites, and short-term variations dominate
4 throughout, while seasonal trends are absent.

5

6 3.3.2 Nocturnal CO₂ fluxes

7 The NSR method requires one representative CO₂ flux value for each night. This value was
8 obtained as the mean of the half-hourly fluxes from the gap-filled EC records. As a quality
9 check on the gap-filling, Fig. 9 compares the night-mean EC fluxes from the complete, gap-
10 filled record with night-means obtained from measured CO₂ fluxes using only runs with
11 $\sigma_w > 0.12 \text{ m s}^{-1}$ (including only nights with at least 9 such runs available). At both sites, and
12 for all seasons, the two time series track each other well. The measured-only series appears at
13 times more scattered, but no systematic differences occur.

14 For the period from 23 September 2013 to 31 March 2014, mean nocturnal CO₂ fluxes at the
15 IFR site were also computed from the respiration chamber data. The ratio of the night-mean
16 EC fluxes to night-mean chamber fluxes was on average 0.87 (± 0.34 SD), and agreement was
17 generally best for the first few days following grazing events (matched by cutting of the grass
18 in the chambers).

19

20 3.3.3 Footprint considerations and nocturnal fluxes of CH₄ and N₂O

21 From footprint models it is known that the source area influencing a flux measurement in the
22 atmospheric surface layer has a larger extent when stratification is stable than when it is
23 unstable (Schmid, 1994; Kormann and Meixner, 2001). During nocturnal low-wind periods,
24 stable stratification prevails, and so, comparatively large source areas can be expected for the
25 NSR method. Further, the source area influencing a mole-fraction measurement extends
26 farther than that influencing a flux measurement (Schmid, 1994). Since the NSR method
27 combines measurements of a flux, that of CO₂, with measurements of the changes of a mole
28 fraction, that of χ , over time, it can be hypothesised that its effective source area is somewhat
29 larger than that of a direct flux measurement (e.g., by eddy covariance or the GGR method).
30 For our setup geometry (Fig. 1), NSR measurements at the IFR site could in part be

1 influenced by conditions over the dryland area, for wind directions either side of N, from 284°
2 to 76°. Similarly, NSR measurements at the UUW site could in part be influenced from either
3 of the two irrigated circles to the S and W, hence for any wind direction between 93° and
4 321°. Table 2 shows the differences in the median nocturnal fluxes between including and
5 excluding periods with winds from the specified directional sectors, as well as the number of
6 nights contributing to each median flux, N . The wind-direction filter is applied on a half-
7 hourly basis, together with the low-turbulence filter ($\sigma_w < 0.12 \text{ m s}^{-1}$), prior to the NSR
8 regression and the filtering for $R^2 > 0.4$ and $n \geq 4$.

9 One effect of the exclusion of unsuitable wind directions is a considerable reduction of N , by
10 about half. In addition (not shown), the number of runs contributing to each night, n , is also
11 on average reduced. Of all nocturnal half-hours with low turbulence, 63 % had unsuitable
12 wind direction for the IFR site, and 67 % for the UUW site. The reason for such high
13 exclusion rates is a predominance of wind from the NW sector, due to katabatic flow from the
14 Southern Alps. Unfortunately, those wind directions that were unsuitable at both sites (284° to
15 321°) were also the most common.

16 At the IFR site, the median CH₄ flux with wind-direction filtering is 3 % greater than without,
17 and the median N₂O flux with filtering is 5 % greater than without. At the UUW site, wind-
18 direction filtering reduces the median CH₄ flux by 38 % and the median N₂O flux by 27 %.
19 The effect of the filter at this site appears large enough to justify its application, despite the
20 considerable reduction in data yield.

21 At both sites and for both gases, the means of the nocturnal fluxes were greater than their
22 medians, with SDs between 0.76 and 1.3 times the mean values. Due to these large relative
23 SDs, the means were quite sensitive to the presence (or exclusion) of outliers and are for that
24 reason not reported in Table 2.

25

26 3.3.4 Uncertainty of the CH₄ and N₂O fluxes

27 The uncertainty of the NSR regression slope is expressed as its standard error (SE). In relative
28 terms, this ranged from 2 % to 80 % of the regression slope, for both sites and gases. For CH₄,
29 the median relative errors of the slopes were 29 % at both sites. For N₂O, these median errors
30 amounted to 20 % at the IFR site and 17 % at the UUW site.

1 The uncertainty of the nocturnal CO₂ fluxes, from the gap-filled EC data, was specified as the
2 SEM for each night. This includes the contributions from random measurement error and
3 temporal variability during the night. Expressed as a relative error, it ranged from 0.4 % to
4 33 % of the flux but rarely exceeded 15 %. The median relative errors were 4.2 % and 4.3 %
5 for the IFR and the UUW site, respectively. The number of runs per night contributing to the
6 mean had a median of 21, at both sites. Multiplying the median relative error of the night-
7 mean flux with 21^{1/2}, the typical relative error of the individual half-hour flux is obtained as
8 19 % and 20 % for the IFR and the UUW site. This appears realistic, since nocturnal CO₂ flux
9 errors in windy conditions are often estimated to be of order 20 % (Moncrieff et al., 1996).

10 We thus estimate the SEM of the nocturnal CH₄ and N₂O fluxes by combining the SEM of the
11 nocturnal CO₂ fluxes with the SE of the regression slopes (using standard root-mean-square
12 propagation). The fluxes and their SEM are shown in Figs. 6 and 7, along with their
13 counterparts from the GGR method.

14

15 **3.4 Combination of GGR and NSR methods**

16 3.4.1 Comparison of the two methods

17 The GGR method provided a higher yield of daily flux values for CH₄ and N₂O than the NSR
18 method, but also the larger day-to-day variability (Figs. 6, 7). The N₂O fluxes from the NSR
19 method generally followed the trends of those from the GGR method well, at timescales of a
20 few days or longer. The same was true for the CH₄ fluxes at the UUW site (Fig. 7), with the
21 exception of a couple of high outliers in Nov 2012 and Jan 2013. For N₂O, the median fluxes
22 from the two methods were also in good agreement (for NSR 23 % and 4 % greater than for
23 GGR at the IFR and the UUW site, respectively).

24 About half of the CH₄ fluxes from the NSR method at the IFR site were considerably greater
25 than those from the GGR method, while the other half agreed well with the trend of the latter
26 (Fig. 6). The likely cause of the discrepancies for CH₄ is the presence of the cattle herd
27 elsewhere in the irrigated circle, acting as a strong source of CH₄ that was not uniformly
28 spread across the pasture surface in the same way as the sources of CO₂ and N₂O. During
29 stable surface-layer stratification, the CH₄ (and CO₂) emitted by the cattle would accumulate

1 in the surface layer and, with mean wind close to zero, slowly spread in all directions until,
2 eventually, being moved and dispersed by an intermittent flow event.

3 Without records of grazing events in paddocks other than those two containing our instrument
4 sites, there are no clear criteria to decide in which nights the NSR estimates of CH₄ flux are
5 significantly biased by cattle emissions and in which they are not. Histograms of the CH₄
6 fluxes for both sites (not shown) suggest that fluxes greater than 80 nmol m⁻² s⁻¹ are very
7 likely outliers due to cattle emissions. We thus remove these from further analysis. This
8 reduces the number of nights, of 101 and 96 for IFR and UUW site (Table 2), to 88 and 95,
9 respectively. However, the possibility remains that further nights are affected and that the
10 NSR estimates for CH₄ fluxes may be overestimated in these.

11

12 3.4.2 Construction of emissions budgets

13 The time series of daily CH₄ and N₂O fluxes can be used to construct emissions budgets for
14 longer periods, such as seasons or years. For this, we wish to make good use of the two
15 complementary methods. A simple approach is to take separate means for the GGR and the
16 NSR method and then average these, giving equal weight to each method (we shall call this
17 the “combined” approach). An alternative approach can be described as follows: first, average
18 GGR and NSR means on a daily basis for each 24-h period in which both estimates are
19 available; then, for 24-h periods in which only one method produced a valid mean flux, use
20 that flux; finally, take the overall mean of this merged time series (we shall call this the
21 “merged” approach). The merged approach gives more weight to the method with the greater
22 data yield.

23 We explore these two approaches for the first year of the dataset (17 August 2012 to
24 16 August 2013). With both approaches, we estimate the uncertainty by propagating the SE of
25 all day-means/night-means into an SE value for the annual mean flux. The results are
26 summarised in Table 3. All flux values in the table are positive, indicating net annual
27 emissions of the two trace gases. Data yields (*N*) are included in the table; for the combined
28 approach no *N* column is given because the individual *N* for the GGR and NSR method apply.

29 For CH₄ at the IFR site, the NSR method estimates 5 times greater emissions than the GGR
30 method, despite the outlier-filtering described above. Since the data yield of the GGR method
31 was 3 times greater, the relative weighting of the two methods matters; consequently, the

1 combined approach results in an emissions estimate that is 1.6 times that of the merged
2 approach. By contrast, for CH₄ at the UUW site, GGR and NSR estimates differ by less than a
3 factor 2; consequently, the combined and merged approach agree within 10 %.

4 For N₂O at the IFR site, the annual NSR mean exceeds the annual GGR mean by a factor 2.6.
5 This is a considerably greater difference than was found for the medians (of this year as well
6 as of the whole dataset). The GGR mean includes 62 % of the days of the year, while the NSR
7 mean is based on 38 % of all nights. Both datasets are evenly spread across the seasons
8 (Fig. 6). The GGR dataset contains a surprisingly large number of negative daily values in
9 Dec 2012 and Jan 2013 while the NSR dataset does not contain negative values, and the
10 different annual means for the two methods are largely caused by this. The combined
11 approach results in an annual flux estimate that is 23 % greater than the estimate from the
12 merged approach, in which the NSR data have less weight.

13 For N₂O at the UUW site, the annual NSR mean exceeds the annual GGR mean by 57 %.
14 Again, this is a greater difference than that for the medians. The data yields for both methods
15 are smaller than at the IFR site, but roughly in the same proportion with each other. The
16 combined approach results in a 5 % greater annual flux estimate than the merged approach,
17 and the ranges indicated by the propagated daily SE are marginally overlapping. Again, the
18 GGR dataset contains some negative daily means (while the NSR dataset does not); these
19 occurred mostly in Oct-Nov 2012, not at the same time as for the IFR site.

20

21

22 **4 Discussion**

23 **4.1 Performance of the GGR method**

24 The GGR and NSR method exploit complementary datasets: for the former, only runs are
25 used in which a set turbulence threshold is exceeded, for the latter only runs in which the
26 opposite is true. The data yield of each method is thus dependent on the general wind climate
27 of the site. However, each method also requires careful screening with other suitability
28 criteria. For the GGR method, we have demonstrated that the main one is to ensure that the
29 mole-fraction gradients of the reference gas (here CO₂) are a few times larger than instrument
30 resolution, in order to contain random scatter within tractable limits. An implication of this

1 requirement is that very high wind speeds tend to be less suitable than moderate wind speeds,
2 because the former dilute emitted gases more quickly and thus reduce their gradients. The
3 exact choice of filtering criteria must balance reliability (constraining random error) with
4 availability (obtaining enough data coverage).

5 Even with appropriate filtering, run-to-run variability of the GGR method is large, because
6 the random errors of three measured variables (two gas mole-fraction gradients and the
7 reference gas flux) combine, and partly because the two gas mole fractions are measured
8 sequentially, not simultaneously (although usage of ballast volumes reduces the effects of
9 timing mismatch somewhat). The random error of a daily mean flux depends, then, on the
10 number of acceptable runs, and may thus be large on some days and small on others. In our
11 experiment, we obtained acceptable daily mean fluxes for approximately 40 % of all days at
12 one site and 60 % at the other. This was sufficient for adequate coverage of all seasons and
13 the estimation of annual budgets of gas emissions.

14 The large uncertainty of individual runs found with the GGR method is similar to that found
15 with the momentum-based aerodynamic method (Phillips et al., 2007). The data yield of the
16 former is probably smaller than that of the latter, because suitably-large [CO₂] gradients
17 (required for GGR) may occur somewhat less often than reliable measurements of friction
18 velocity (required for the aerodynamic method). However, the GGR method avoids any
19 assumptions on Schmidt number and stability dependence and its diffusivity estimates are
20 therefore more defensible for the purpose of computing trace gas fluxes.

21 For both trace gases, negative flux values (uptake) were occasionally observed with the GGR
22 method. In the case of CH₄, the negative fluxes were spread across all seasons, at both sites.
23 They are thus considered as manifestations of the large random variability. By contrast,
24 negative fluxes of N₂O were occasionally clustered in certain periods. These cluster periods
25 were not synchronous at the two sites. During these, the mole-fraction gradients with reversed
26 sign occurred consistently over many successive cycles, suggesting that they had a true cause,
27 rather than occurring randomly. However, the NSR method did not indicate N₂O uptake
28 during these periods. While we cannot rule out the possibility that the negative N₂O fluxes
29 from the GGR method were artefacts, we have no indication from the data themselves, or our
30 records of instrument operation and farm management, why they might have been.

31

1 **4.2 Performance of the NSR method**

2 The NSR method relies on the occurrence of nocturnal calm periods of a few hours duration.
3 Such periods do not occur every night. When they do, the method is technically robust, since
4 the gas mole-fraction changes over time tend to be large and can be well-resolved. A crucial
5 assumption of the NSR method is the co-location, in space and time, of the sources or sinks of
6 the trace gas of interest and the reference gas. In our experiment, the results for N₂O were
7 very consistent with those from the GGR method, so we conclude that for N₂O and CO₂ over
8 pasture this assumption holds well enough, as it did in the pioneering experiment of Kelliher
9 et al. (2002). The results for CH₄ were less consistent, and we attribute that to the presence of
10 cow herds in the larger surroundings of the measurement site. These constituted strong
11 additional sources, of both CH₄ and CO₂ but with a very different emissions ratio to that valid
12 for the pasture, and therefore occasionally (depending on intermittent winds) impacting on the
13 correct retrieval of the latter.

14 The footprint of the NSR method has a rather large spatial extent, compared to the GGR
15 method. Because of the requirement of co-location of sources/sinks, one needs to exclude
16 periods when the extension of the target surface in the wind direction is too short. In our
17 experiment, the prevalence of katabatic flow from a certain directional sector led to the
18 exclusion of 40 % or more of otherwise suitable calm nights. Such high exclusion rates could
19 be avoided by maximising the fetch in the main regional upslope direction (but in our case,
20 this would have conflicted with the requirements of the dual-site setup and was thus
21 impossible). Here, the NSR method provided fewer night-mean flux estimates than the
22 number of daily means obtained with the GGR method; however, this does not need to be the
23 case in general, since the data yield of both methods depends on local wind climate and
24 footprint considerations.

25 The NSR method requires reliable flux estimates for the reference gas. We have here explored
26 a novel approach to this end, by using gap-filled long-term time series of CO₂ flux records,
27 instead of chamber measurements. Hence, the actual flux values used for the NSR-suitable
28 nighttime periods were modelled, but strongly based on measured fluxes in the surrounding
29 windier periods. They were validated against chamber measurements and found to provide
30 adequate estimates of the nocturnal mean respiration flux, with a relative uncertainty that was
31 usually smaller than that of the NSR regression slope and therefore did not impact negatively
32 on the success of the NSR method.

1

2 **4.3 Annual means of CH₄ and N₂O emission rates**

3 Either of the two methods, GGR and NSR, can provide annual budget estimates of trace gas
4 fluxes on its own, provided that these fluxes do not undergo strong systematic diurnal
5 variations. If they did, then biases would be likely, since the GGR method yields more data
6 during the day than at night and the NSR method is explicitly nocturnal only. We thus
7 strongly recommend to combine the two methods. As they are applicable in mutually-
8 exclusive conditions (well-developed turbulence and calm, respectively), their combination
9 optimises data usage.

10 We tested two approaches to combine the GGR and NSR results: either combining their
11 separate annual means, or merging the two time series into one before computing a joint
12 annual mean. Ideally, the two approaches should not differ by much. Here, we found that to
13 be the case for the CH₄ fluxes at the UUW site. However, when the results from the GGR and
14 NSR methods show systematic differences, then some operator judgment is required whether
15 that reflects true day-night differences of the fluxes or whether one of the two methods is
16 likely to be biased. In the former case, combining GGR and NSR means would be adequate,
17 as that would give similar weights to daytime and nighttime data. In the latter case, the likely
18 cause of bias needs to be assessed and the decision how to weigh the GGR and NSR results
19 must be based on that assessment.

20 For the CH₄ results at the IFR site, we suspect that the mean fluxes from the NSR method are
21 overestimated in many nights, due to the presence of cows emitting CH₄ elsewhere on the
22 irrigated-pasture circles. Thus, for CH₄ we decide to give high weight to the GGR method, by
23 using the results from the merged approach. This yields identical emission rates of
24 $8.9 (\pm 0.79) \text{ nmol m}^{-2} \text{ s}^{-1}$ for the two sites (Table 3). If we used the combined approach
25 instead, the mean emission rate from the IFR site would appear as the significantly greater
26 one.

27 For annual N₂O fluxes, the mean from the NSR method was somewhat greater than that from
28 the GGR method, at both sites. We found the differences to originate mainly from certain
29 periods in which the GGR method repeatedly indicated negative fluxes, while the NSR
30 method did not. It is possible that during these periods the pasture acted as an N₂O sink during
31 daytime and as a source during the night; Hörtnagl and Wohlfahrt (2014) observed such

1 behaviour in the spring seasons of two consecutive years and in autumn for one of these
2 years. Therefore, we decide to use the combined approach for N₂O, giving equal weight to the
3 GGR and NSR method despite the greater data yield of the former. Considering high N₂O
4 fluxes as undesirable, this decision errs on the side of caution and produces somewhat greater
5 emission rates than would be obtained with the merged approach. These emission rates are
6 0.58 (±0.020) and 0.38 (±0.018) nmol m⁻² s⁻¹ for the IFR and the U UW site, respectively
7 (Table 3). Hence, the emission rates from the IFR site were significantly greater than those
8 from the U UW site, by 53 %. This is in line with expectations, given the greater N inputs
9 from fertiliser application and excreta deposition at the IFR site.

10

11 **4.4 CH₄ fluxes from managed grasslands**

12 Agricultural soils, when not waterlogged, are expected to be weak sinks for CH₄ (Smith et al.,
13 2003), and chamber studies have tended to confirm this expectation. For example, Imer et al.
14 (2013) reported net uptake rates for three managed ungrazed grassland sites in Switzerland;
15 Savage et al. (2014) found annual CH₄ uptake of 0.2 g C m⁻² for an alfalfa field in North
16 Dakota, using year-round auto-chamber sampling. In New Zealand, Li and Kelliher (2007)
17 reported net uptake rates of 0.14 and 0.05 g C m⁻² yr⁻¹ for a well-drained and a poorly-
18 drained dairy-pasture soil, situated 300 m apart. By contrast, the results reported here indicate
19 both the IFR and the U UW site to be CH₄ sources, with similar annual net emissions (for the
20 year starting 17 August 2012) of 3.4 g C m⁻². Even if one discarded the NSR results
21 completely on suspicion of CH₄ contamination by animal herds in the wider surroundings, the
22 GGR datasets alone still have positive means and medians, at both sites. Since the daytime
23 footprint extensions for the GGR method were of order 300 m or less, we can be confident
24 that the GGR results were generally representative for pasture surfaces free of grazing
25 animals.

26 Other micrometeorological studies of grasslands are useful to compare with our CH₄ results
27 only where grazing events were excluded from the data, where the soils were not peaty and
28 where the footprint contained no open water surfaces. Using eddy covariance, Hörtnagl and
29 Wohlfahrt (2014) found, at an alpine meadow that was cut three times per year, CH₄ emission
30 rates of order 1 nmol m⁻² s⁻¹; these were very consistent throughout all snow-free seasons.
31 For a grassland site after restoration, Merbold et al. (2014) report annual CH₄ emissions of

1 3.53 g C m⁻², very similar to our two sites, and daily mean emissions were in the majority of
2 positive sign in every month. Griffith et al. (2002), using the flux-gradient method over
3 lucerne pasture in New South Wales, reported mean and median daytime fluxes of 2.95 and
4 2.85 nmol m⁻² s⁻¹, and even though these were not significantly different from zero due to the
5 short duration of that experiment (3 weeks), the sign and magnitude agree with those from the
6 other micrometeorological studies. It appears that net CH₄ emissions from managed
7 grasslands are not uncommon, which is at odds with those chamber experiments that
8 demonstrated CH₄ oxidation. A possible explanation is that frequent N fertilisation inhibits
9 the oxidation process and/or stimulates CH₄-producing microbes in the soil (Price et al.,
10 2004). Li and Kelliher (2007) found that urine application reduced net CH₄ uptake
11 significantly, both for a well-drained and a poorly-drained soil. We note, though, that the net
12 uptake rates observed for each of their treatments were at least one magnitude smaller than the
13 mean emission rates at our sites. The same is true for an experiment with intact soil cores
14 from European sites (Schaufler et al., 2010), where the cropland and grassland soils showed
15 CH₄ fluxes smaller than 0.06 nmol m⁻² s⁻¹, some with net uptake and some with net
16 emissions, and without dependence on soil moisture or temperature. Another possible factor
17 favouring CH₄ emissions may be the soil compaction caused by intensive grazing events,
18 provided that leads to an increased occurrence of anaerobic microsites in the soil. Whatever
19 the exact mechanisms, the field-scale CH₄ flux measurements here and elsewhere suggest that
20 on managed pastures, CH₄ oxidation rates in the soil can be overwhelmed by concurrent
21 emission processes.

22

23 **4.5 N₂O emissions and nitrogen inputs**

24 The time series of N₂O fluxes in Figs. 6 and 7 are, overall, relatively steady. In Fig. 6, there is
25 no quasiperiodic pattern that would indicate a response to events of strong N input (grazing or
26 fertilisation). There is also an almost complete lack of strong episodic events. Such events
27 have often been reported to closely follow rainfall or irrigation events (e.g. van der Weerden
28 et al., 2013), and they are found to occur in a relatively narrow range of soil moisture that is
29 site-specific. Balaine et al. (2013) present evidence that the driving variable for peak N₂O
30 emissions is the relative soil gas diffusivity. Here, at the IFR site throughout the milking
31 season, it appears that VWC was generally too low to reach the conditions required for peak
32 emissions. The highest VWC occurred over winter 2013 (June to August), generally between

1 0.4 and 0.55 m³ m⁻³ (equivalent to 60 and 83 % water-filled pore space, respectively, given a
2 porosity of 66 % in the soil layer from 0 to 10 cm depth). During this winter period, the N₂O
3 fluxes appeared particularly small and steady, at 0 to 0.5 nmol m⁻² s⁻¹. This was also a period
4 in which no fertilisation or grazing events occurred. The relative steadiness of N₂O emission
5 rates throughout all seasons is probably largely due to the well-drained soil. This feature
6 distinguishes this intensively managed pasture site from others (Phillips et al., 2007) where
7 emissions were of a more episodic nature and more obviously responding to irrigation events.

8 In Table 4, we relate the N₂O emissions at the IFR site to the N inputs, for the same year as in
9 Table 3. The N inputs are obtained as follows. Fertilisers were applied by a certified
10 commercial contractor who recorded the amounts per area; we assume a relative error of 7 %
11 from expert judgment. The N inputs from cattle excreta can be accounted for as the N intake
12 by the animals reduced by the N retention in liveweight and the N content of milk produced,
13 under the assumption that all excreted N is returned to the irrigated-pasture circle either in-
14 situ as dung and urine or by effluent application. Following Hunt et al. (2016), the dry-matter
15 intake of the cattle herd for the 2012/13 milking season was 1.167 (±0.026) kg m⁻² (90 %
16 grazed pasture, 10 % barley supplements). With an N content of 2.7 (±0.2) % for
17 ryegrass/clover pasture (Mills and Moot, 2010), the N intake amounted to
18 31.5 (±2.4) g N m⁻². The total liveweight gain of the herd over the milking season was
19 estimated as 52,200 kg, based on national statistics (DairyNZ, 2013) and the age structure of
20 the herd. Dividing by the total grazed area of the farm (328 ha), and assuming an N content of
21 3.6 % for meat (AMC, 2014), the N retention in liveweight per pasture area was 0.57 g N m⁻²
22 (1.8 % of N intake). The milk production of the farm for 2012/13 was 3.96 * 10⁶ L. Assuming
23 that the milk contained 5.8 (±0.5) g N L⁻¹ (Woodward et al., 2011), the amount of N exported
24 in milk was 7.0 (±0.6) g N m⁻² (22 % of N intake). The amount of N returned in excreta thus
25 results as 23.9 (±2.5) g N m⁻².

26 The figure for the N₂O emissions in Table 4 comes from the combined approach (see Section
27 4.3), converted from molar units (0.58 nmol m⁻² s⁻¹) to mass units and integrated over a year,
28 yielding 0.51 g N m⁻². The uncertainty of this value is assumed as 10 % in relative terms. This
29 is greater (about 3 times) than the propagated SE in Table 3, partly to account for the
30 mismatch between approaches as discussed above, and partly to allow for the possibility that
31 the spatial variability in the whole irrigated circle may have been larger than in the footprint
32 of our measurement site. Dividing the N₂O emissions by the N inputs, the emission factor

1 results as 1.21 (± 0.15) %. We consider this as an upper estimate because some fraction of the
2 measured emissions may be natural background emissions. In a chamber experiment in
3 February/March 2014, N₂O fluxes from the control plots (which were irrigated but received
4 no N) were consistently about 0.5 mg N m⁻² d⁻¹, over 35 d, (Jennifer Owens, pers. comm.).
5 Integrated over a year, this would amount to 0.18 g N m⁻². If we tentatively use this value as
6 “background” emissions (even though a fraction of it may still have occurred in response to
7 preceding fertilisations), then the net N₂O emissions above background would have been
8 0.33 g N m⁻² and the emission factor 0.78 %. This value is very close to the mean emission
9 factor for dairy cattle excreta, of 0.73 %, from a statistical analysis of 125 field trials in New
10 Zealand (Kelliher et al., 2014). With or without the background included, the observed
11 emission factor is also compatible with the value of 1 % recommended for national
12 greenhouse-gas inventories (IPCC, 2006).

13 At the U UW site, there was no fertiliser applied during the year starting 17 Aug 2012. There
14 was one winter grazing by 200 cattle in May; Fig. 7 shows a few elevated points in the time
15 series of the N₂O flux that may have occurred in response to that. There had also been a
16 winter grazing in June 2012, before our recording began. Some of the observed emissions
17 early in the budget year would have originated from the N deposited during that event,
18 possibly amplified by the effects of trampling (Pal et al., 2014). It is therefore likely that the
19 annual emissions at the U UW site, of 0.34 g N m⁻², were also greater than natural background
20 emissions.

21 The annual N₂O emissions at our two sites are comparable to those from grassland sites
22 elsewhere in the world. Phillips et al. (2007) measured N₂O fluxes from flood-irrigated,
23 rotationally-grazed pasture in SE Australia. For two consecutive years, they obtained annual
24 emissions of 0.55 and 0.44 g N m⁻², respectively, bracketing the result for the IFR site.
25 Burchill et al. (2014) found, for a rotationally-grazed and intensively fertilised ryegrass
26 pasture in Ireland, annual N₂O emissions over 4 years to range from 0.44 to 3.44 g N m⁻². The
27 annual emissions from the IFR site are within this range, near the lower end. Burchill et al.
28 (2014) also measured the annual emissions from ungrazed, unfertilised ryegrass pasture.
29 These ranged from 0.17 to 0.63 g N m⁻², i.e. from about half to about twice the annual
30 emissions from the U UW site. Soussana et al. (2007) reported annual N₂O emissions from
31 10 European grassland sites to range from -0.025 to 0.687 g N m⁻²; management practices

1 and fertiliser application rates at these sites varied considerably. Imer et al. (2013) found
2 annual emissions for three managed ungrazed grassland sites from 0.13 to 1.13 g N m⁻².

3

4 **4.6 Comparison to other methods**

5 Traditionally, the most common methods to measure trace gas fluxes from or to soils and
6 vegetation have been chamber methods. Their main advantages are high accuracy of the
7 individual sampling, and often low costs (Denmead, 2008). One of their main drawbacks is
8 limited coverage in time (due to operational constraints), though modern autochamber
9 systems with robust field-worthy gas analysers are largely overcoming this disadvantage (van
10 der Weerden et al., 2013; Savage et al., 2014). The other main drawback is that they do not
11 operate at the field scale, which is of particular relevance where gas emissions occur highly
12 concentrated from preferential spots, such as patches of animal excreta. Micrometeorological
13 methods, by contrast, integrate over this spatial variability, and they are in principle
14 continuous in time, except for certain filtering requirements, such as for unsuitable wind
15 direction or insufficient turbulence.

16 For CH₄ and N₂O, the most commonly used micrometeorological method nowadays is eddy
17 covariance, thanks to the advent of a number of fast and precise gas analysers based on laser
18 technologies. Drawbacks of EC are that these analysers are expensive and must be dedicated
19 to a single site, that there are often issues with instrument noise and signal resolution,
20 particularly when fluxes are small for extended periods, and that for periods of small fluxes,
21 the accuracy depends strongly on corrections for density effects and cross-sensitivities (Neftel
22 et al., 2010). Since EC relies on stationary turbulent flow in the surface layer, data from calm
23 nights must be discarded. In this respect, EC is very similar to the GGR method and other
24 variants of flux-gradient methods. Our approach to combine precise mole-fraction
25 measurements of trace gases of interest with EC measurements of CO₂ offers the following
26 advantages over direct EC measurements of the trace gases. First, it allows to measure at
27 more than one site with the same gas analyser (provided the sites are not too far apart).
28 Second, it allows to use a multi-gas analyser, such as the FTIR; in fact this is the ideal choice
29 because the mole fractions of the gas of interest and of CO₂ are measured in the same air
30 sample. Third, by then using GGR and NSR as complementary methods to compute the trace
31 gas fluxes, the sampling includes periods of well-developed and low turbulence and leads to a

1 higher data yield than EC or GGR alone. Of course, the NSR method could potentially also be
2 applied as a complement to direct EC measurements, provided that the EC system includes
3 CO₂ flux measurements (which is routinely the case) and that these are taken close enough to
4 the ground to keep the footprint of the NSR method representative for the surface of interest
5 (which may be less common).

6 The GGR and NSR method each require some optimisation of data filtering criteria: the GGR
7 method for sufficient resolution of CO₂ mole-fraction gradients and positive gas diffusivities,
8 and the NSR method for reliability of nocturnal linear regressions and possibly for suitable
9 wind direction (site-dependent). These criteria appear relatively straightforward, compared to
10 the suite of data quality filters required for the eddy-covariance method. Further, the GGR and
11 NSR method each employ simple algebraic relationships for gas ratios, which do not require
12 further corrections; in this, they are easier to implement than the eddy-covariance method
13 with its rather complex correction procedures involved in the computation of minor trace gas
14 fluxes.

15

16

17 **5 Conclusions**

18 Continuous year-round measurements of the fluxes of CH₄ and N₂O at two neighbouring,
19 contrasting pasture sites were obtained with the combination of GGR and NSR methods, both
20 using CO₂ as the reference gas (tracer). The CH₄ and N₂O fluxes resembled those from other
21 managed grasslands measured with the eddy-covariance or the flux-gradient method. The
22 combination of GGR and NSR methods can thus serve as a viable alternative to eddy
23 covariance and is particularly attractive in paired-site setups. However, the NSR method
24 should be applied with caution for trace gases that have strong sources or sinks not co-located
25 with those for the reference gas. Land-use patterns in the surrounding area, as well as regional
26 topography and climate, therefore influence the yield of usable data.

27 A novelty introduced here, different to the original concept of the NSR method (Kelliher et
28 al., 2002), is the usage of gap-filled CO₂ flux time series from eddy covariance, instead of
29 CO₂ fluxes from respiration chambers. Mean nocturnal CO₂ fluxes from this approach agreed
30 well with those from chambers, proving its validity.

1 For N₂O, the fluxes obtained with the GGR and NSR method were in reasonable agreement
2 with each other, and they were also fully compatible with the results from a wealth of
3 chamber studies and with recommended emission factors for N₂O emissions from dairy
4 pasture. The combination of GGR and NSR is thus a reliable option to obtain long-term
5 budgets of the N₂O exchange of ecosystems on flat land, with the advantage of effective
6 spatial integration of the source area (which is not guaranteed for chamber systems).

7 For CH₄, both the GGR and NSR method indicated net emissions from both pasture sites.
8 These were similar to emissions at other grassland sites measured with micrometeorological
9 methods. However, chamber measurements on grassland often show CH₄ fluxes that are one
10 or two magnitudes smaller and in the opposite direction, indicating CH₄ oxidation in the soil.
11 It is at this stage unclear whether these discrepancies have their origin in the different
12 methods (e.g. the different spatial coverage with chambers and micrometeorological methods)
13 or in different management practices (e.g. fertilisation amounts and frequency, disturbance
14 from animal treading).

15

16

17 **Acknowledgements**

18 We are grateful to Tony McSeveny and Graeme Rogers for immense technical support in the
19 field, Graham Kettlewell (University of Wollongong) for technical assistance with the FTIR,
20 and the owner of Beacon Farm, Synlait Farms Co. (now renamed to Purata), for supporting
21 our research. We thank Gabriel Moinet for contributing his respiration chamber data to assess
22 nocturnal CO₂ fluxes, and Jennifer Owens for sharing her N₂O chamber results. This research
23 was undertaken with CRI Core Funding from New Zealand's Ministry of Business, Innovation
24 and Employment.

25

26

27

1 References

- 2 Acevedo, O. C., Moraes, O. L. L., Degrazia, G. A., Fitzjarrald, D. R., Manzi, A. O., and Campos, J.
3 G.: Is friction velocity the most appropriate scale for correcting nocturnal carbon dioxide
4 fluxes? *Agric. For. Meteorol.*, 149, 1-10, 2009.
- 5 AMC (Analytical Methods Committee): Meat and poultry nitrogen factors. *Anal. Methods*, 6, 4493-
6 4495, 2014.
- 7 Balaine, N., Clough, T. J., Beare, M. H., Thomas, S. M., Meenken, E. D., and Ross, J. G.: Changes in
8 relative gas diffusivity explain soil nitrous oxide flux dynamics, *Soil Sci. Soc. Am. J.*, 77, 1496-
9 1505, 2013.
- 10 Baldocchi, D.: Measuring fluxes of trace gases and energy between ecosystems and the atmosphere -
11 the state and future of the eddy covariance method, *Global Change Biology*, 20, 3600-3609,
12 2014.
- 13 Burchill, W., Li, Dejun, Lanigan, G. J., Williams, M., and Humphreys, J.: Interannual variation in
14 nitrous oxide emissions from perennial ryegrass/white clover grassland used for dairy
15 production, *Global Change Biology*, 20, 3137-3146, 2014.
- 16 DairyNZ: New Zealand Dairy Statistics 2012-2013. DairyNZ and Livestock Improvement
17 Corporation, Hamilton, New Zealand, 52 pp., [http://www.lic.co.nz/user/file/
18 DAIRY%20STATISTICS%202012-13-WEB.pdf](http://www.lic.co.nz/user/file/DAIRY%20STATISTICS%202012-13-WEB.pdf), 2013 (accessed 16 December 2015).
- 19 Denmead, O. T.: Approaches to measuring fluxes of methane and nitrous oxide between landscapes
20 and the atmosphere, *Plant and Soil*, 309, 5-24, 2008.
- 21 Eamus, D., Cleverly, J., Boulain, N., Grant, N., Faux, R., and Villalobos-Vega, R.: Carbon and water
22 fluxes in an arid-zone *Acacia* savanna woodland: An analyses of seasonal patterns and
23 responses to rainfall events, *Agric. For. Meteorol.*, 182-183, 225-238,
24 doi:10.1016/j.agrformet.2013.04.020, 2013.
- 25 Eugster, W., Zeyer, K., Zeeman, M., Michna, P., Zingg, A., Buchmann, N., and Emmenegger, L.:
26 Methodical study of nitrous oxide eddy covariance measurements using quantum cascade laser
27 spectrometry over a Swiss forest, *Biogeosciences*, 4, 927-939, doi:10.5194/bg-4-927-2007,
28 2007.
- 29 Felber, R., Munger, A., Neftel, A., and Ammann, C.: Eddy covariance methane flux measurements
30 over a grazed pasture: effect of cows as moving point sources, *Biogeosciences*, 12, 3925-3940,
31 doi:10.5194/bg-12-3925-2015, 2015.
- 32 Griffith, D. W. T., Leuning, R., Denmead, O. T., and Jamie, I. M.: Air-land exchanges of CO₂, CH₄
33 and N₂O measured by FTIR spectrometry and micrometeorological techniques, *Atmos.*
34 *Environ.*, 36, 1833-1842, 2002.
- 35 Griffith, D. W. T., Deutscher, N. M., Caldow, C., Kettlewell, G., Rikkenbach, M., and Hammer, S.: A
36 Fourier transform infrared trace gas and isotope analyser for atmospheric applications, *Atmos.*
37 *Meas. Tech.*, 5, 2481-2498, doi:10.5194/amt-5-2481-2012, 2012.

- 1 Hörtnagl, L., and Wohlfahrt, G.: Methane and nitrous oxide exchange over a managed hay meadow,
2 Biogeosciences, 11, 7219-7236, doi:10.5194/bg-11-7219-2014, 2014.
- 3 Hsu, K.-I., Gupta, H. V., Gao, X., Sorooshian, S., and Imam, B.: Self-organizing linear output map
4 (SOLO): An artificial neural network suitable for hydrologic modeling and analysis, Water
5 Resources Res., 38, 1302, doi:10.1029/2001wr000795, 2002.
- 6 Hunt, J. E., Laubach, J., Barthel, M., Fraser, A., and Phillips, R. L.: Carbon budgets for an irrigated
7 intensively-grazed dairy pasture and an unirrigated winter-grazed pasture, submitted to
8 Biogeosciences, this issue, 2016.
- 9 Imer, D., Merbold, L., Eugster, W., and Buchmann, N.: Temporal and spatial variations of soil CO₂,
10 CH₄ and N₂O fluxes at three differently managed grasslands, Biogeosciences, 10, 5931-5945,
11 doi:10.5194/bg-10-5931-2013, 2013.
- 12 IPCC: Emissions from livestock and manure management. In: Guidelines for National Greenhouse
13 Gas Inventories, Chapter 10. Intergovernmental Panel on Climate Change, 87 pp.
14 http://www.ipcc-nggip.iges.or.jp/public/2006gl/pdf/4_Volume4/V4_10_Ch10_Livestock.pdf,
15 2006.
- 16 Kelliher, F. M., Reisinger, A. R., Martin, R. J., Harvey, M. J., Price, S. J., and Sherlock, R. R.:
17 Measuring nitrous oxide emission rate from grazed pasture using Fourier-transform infrared
18 spectroscopy in the nocturnal boundary layer, Agric. For. Meteorol., 111, 29-38, 2002.
- 19 Kelliher, F. M., Cox, N., van der Weerden, T. J., de Klein, C. A. M., Luo, J., Cameron, K. C., Di, H.
20 J., Giltrap, D., and Rys, G.: Statistical analysis of nitrous oxide emission factors from pastoral
21 agriculture field trials conducted in New Zealand, Environmental Pollution, 186, 63-66, 2014.
- 22 Kormann, R., and Meixner, F. X.: An analytical footprint model for non-neutral stratification.
23 Boundary-Layer Meteorol., 99, 207-224, 2001.
- 24 Kroon, P. S., Hensen, A., Jonker, H. J. J., Zahniser, M. S., Van't Veen, W. H., and Vermeulen, A. T.:
25 Suitability of quantum cascade laser spectroscopy for CH₄ and N₂O eddy covariance flux
26 measurements, Biogeosciences, 4, 715-728, doi:10.5194/bg-4-715-2007, 2007.
- 27 Kroon, P. S., Hensen, A., Jonker, H. J. J., Ouwensloot, H. G., Vermeulen, A. T., and Bosveld, F. C.:
28 Uncertainties in eddy covariance flux measurements assessed from CH₄ and N₂O observations,
29 Agric. For. Meteorol., 150, 806-816, 2010.
- 30 Laubach, J., Kelliher, F. M., Knight, T., Clark, H., Molano, G., and Cavanagh, A.: Methane emissions
31 from beef cattle - a comparison of paddock- and animal-scale measurements, Aust. J. Exp.
32 Agric., 48, 132-137, 2008.
- 33 Laubach, J., Bai, Mei, Pinares-Patiño, C. S., Phillips, F. A., Naylor, T. A., Molano, G., Cárdenas
34 Rocha, E. A., and Griffith, D. W. T.: Accuracy of micrometeorological techniques for detecting
35 a change in methane emissions from a herd of cattle, Agric. For. Meteorol., 176, 50-63, 2013.
- 36 Leahy, P., Kiely, G., and Scanlon, T. M.: Managed grasslands: A greenhouse gas sink or source?,
37 Geophys. Res. Lett., 31, L20507, 2004.

- 1 Li, Z., and Kelliher, F. M.: Methane oxidation in freely and poorly drained grassland soils and effects
2 of cattle urine application, *J. Environ. Qual.*, 36, 1241-1248, 2007.
- 3 McMillan, A. M. S., Goulden, M. L., and Tyler, S. C.: Stoichiometry of CH₄ and CO₂ flux in a
4 California rice paddy, *J. Geophys. Res.*, 112, G01008, 2007.
- 5 Merbold, L., Eugster, W., Stieger, J., Zahniser, M., Nelson, D., and Buchmann, N.: Greenhouse gas
6 budget (CO₂, CH₄ and N₂O) of intensively managed grassland following restoration, *Global
7 Change Biology*, 20, 1913-1928, 2014.
- 8 MfE: New Zealand's Greenhouse Gas Inventory 1990-2013. Ministry for the Environment,
9 Wellington, New Zealand, 450 pp. [http://www.mfe.govt.nz/publications/climate-change/new-
10 zealands-greenhouse-gas-inventory-1990-2013](http://www.mfe.govt.nz/publications/climate-change/new-zealands-greenhouse-gas-inventory-1990-2013), 2015.
- 11 Mills, A., and Moot, D. J.: Annual dry matter, metabolisable energy and nitrogen yields of six dryland
12 pastures six and seven years after establishment. *Proceedings of the New Zealand Grassland
13 Association*, 72, 177-184, 2010.
- 14 Miyata, A., Leuning, R., Denmead, O. T., Kim, Joon, and Harazono, Y.: Carbon dioxide and methane
15 fluxes from an intermittently flooded paddy field, *Agric. For. Meteorol.*, 102, 287-303, 2000.
- 16 Moncrieff, J. B., Malhi, Y., and Leuning, R.: The propagation of errors in long-term measurements of
17 land-atmosphere fluxes of carbon and water. *Global Change Biology*, 2, 231-240, 1996.
- 18 Montzka, S. A., Dlugokencky, E. J., and Butler, J. H.: Non-CO₂ greenhouse gases and climate change,
19 *Nature*, 476, 43-50, doi:10.1038/nature10322, 2011.
- 20 Mudge, P. L., Wallace, D. F., Rutledge, S., Campbell, D. I., Schipper, L. A., and Hosking, C. L.:
21 Carbon balance of an intensively grazed temperate pasture in two climatically contrasting years,
22 *Agric. Ecosyst. Environ.*, 144, 271-280, 2011.
- 23 Neftel, A., Spirig, C., and Ammann, C.: Application and test of a simple tool for operational footprint
24 evaluations. *Environmental Pollution*, 152, 644-652, 2008.
- 25 Neftel, A., Ammann, C., Fischer, C., Spirig, C., Conen, F., Emmenegger, L., Tuzson, B., and Wahlen,
26 S.: N₂O exchange over managed grassland: Application of a quantum cascade laser
27 spectrometer for micrometeorological flux measurements, *Agric. For. Meteorol.*, 150, 775-785,
28 2010.
- 29 Nicolini, G., Castaldi, S., Fratini, G., and Valentini, R.: A literature overview of micrometeorological
30 CH₄ and N₂O flux measurements in terrestrial ecosystems, *Atmos. Environ.*, 81, 311-319,
31 2013.
- 32 Nieveen, J. P., Campbell, D. I., Schipper, L. A., and Blair, I. J.: Carbon exchange of grazed pasture on
33 a drained peat soil, *Global Change Biology*, 11, 607-618, 2005.
- 34 Oke, T. R., *Boundary Layer Climates*, 2nd ed., Methuen Press, London, 435 pp., 1987.
- 35 Pal, P., Clough, T. J., and Kelliher, F. M.: Sources of N₂O-N following simulated animal treading of
36 ungrazed pastures, *N.Z. J. Agric. Res.*, 57, 202-215, 2014.

- 1 Pendall, E., Schwendenmann, L., Rahn, T., Miller, J. B., Tans, P. P., and White, J. W. C.: Land use
2 and season affect fluxes of CO₂, CH₄, CO, N₂O, H₂ and isotopic source signatures in Panama:
3 evidence from nocturnal boundary layer profiles, *Global Change Biology*, 16, 2721-2736, 2010.
- 4 Phillips, F. A., Leuning, R., Baigent, R., Kelly, K. B., and Denmead, O. T.: Nitrous oxide flux
5 measurements from an intensively managed irrigated pasture using micrometeorological
6 techniques, *Agric. For. Meteorol.*, 143, 92-105, 2007.
- 7 Price, S. J., Kelliher, F. M., Sherlock, R. R., Tate, K. R., and Condon, L. M.: Environmental and
8 chemical factors regulating methane oxidation in a New Zealand forest soil. *Aust. J. Soil Res.*,
9 42, 767-776, 2004.
- 10 Savage, K., Phillips, R., and Davidson, E.: High temporal frequency measurements of greenhouse gas
11 emissions from soils. *Biogeosciences*, 11, 2709-2720, 2014.
- 12 Schaufler, G., Kitzler, B., Schindlbacher, A., Skiba, U., Sutton, M. A., and Zechmeister-Boltenstern,
13 S.: Greenhouse gas emissions from European soils under different land use: effects of soil
14 moisture and temperature, *Europ. J. Soil Sci.*, 61, 683-696, 2010.
- 15 Schmid, H. P.: Source Areas for Scalars and Scalar Fluxes, *Boundary-Layer Meteorol.*, 67, 293-318,
16 1994.
- 17 Schrier-Uijl, A. P., Kroon, P. S., Hendriks, D. M. D., Hensen, A., Van Huissteden, J., Berendse, F.,
18 and Veenendaal, E. M.: Agricultural peatlands: towards a greenhouse gas sink – a
19 synthesis of a Dutch landscape study. *Biogeosciences*, 11, 4559-4576, 2014.
- 20 Smith, K. A., Ball, T., Conen, F., Dobbie, K. E., Massheder, J., and Rey, A.: Exchange of greenhouse
21 gases between soil and atmosphere: interactions of soil physical factors and biological
22 processes, *Europ. J. Soil Sci.*, 54, 779-791, 2003.
- 23 Soussana, J. F., Allard, V., Pilegaard, K., Ambus, P., Amman, C., Campbell, C., Ceschia, E., Clifton-
24 Brown, J., Czobel, S., Domingues, R., Flechard, C., Fuhrer, J., Hensen, A., Horvath, L., Jones,
25 M., Kasper, G., Martin, C., Nagy, Z., Neftel, A., Raschi, A., Baronti, S., Rees, R. M., Skiba, U.,
26 Stefani, P., Manca, G., Sutton, M., Tuba, Z., and Valentini, R.: Full accounting of the
27 greenhouse gas (CO₂, N₂O, CH₄) budget of nine European grassland sites. *Agric. Ecosyst.*
28 *Environ.*, 121, 121-134, 2007.
- 29 Tuzson, B., Hiller, R. V., Zeyer, K., Eugster, W., Neftel, A., Ammann, C., and Emmenegger, L.: Field
30 intercomparison of two optical analyzers for CH₄ eddy covariance flux measurements, *Atmos.*
31 *Meas. Tech.*, 3, 1519-1531, 2010.
- 32 Van der Weerden, T. J., Clough, T. J., and Styles, T. M.: Using near-continuous measurements of N₂O
33 emission from urine-affected soil to guide manual gas sampling regimes, *N.Z. J. Agric. Res.*,
34 56, 60-76, 2013.
- 35 Wilson, J. D.: Turbulent Schmidt numbers above a wheat crop, *Boundary-Layer Meteorol.*, 148, 255-
36 268, 2013.

- 1 Woodward, S. L., Waghorn, G. C., Bryant, M. A., and Mandok, K.: Are high breeding worth index
- 2 cows more feed conversion efficient and nitrogen use efficient? Proceedings of the New
- 3 Zealand Society of Animal Production, 71, 109-113, 2011.
- 4

1 **Tables**

2

3 **Table 1.** Results of repeated mole-fraction measurements, with the FTIR spectrometer, of air
 4 from a gas cylinder with near-ambient composition (quality control). The two switching
 5 cycles are described in Section 2.2.1. Numbers in parentheses are standard deviations, from n
 6 successive cell fills.

7

Switching cycle	n	[N ₂ O] (ppb)	[CH ₄] (ppb)	[CO ₂] (ppm)
Original – 6 min	38	384.07 (0.28)	1805.22 (0.58)	389.53 (0.15)
Modified – 12 min	43	384.53 (0.14)	1808.04 (0.20)	389.79 (0.12)

8

9

10

11 **Table 2.** Medians of nocturnal fluxes computed with the NSR method, as well the number of
 12 nights (N) contributing to the median, for two wind-direction selections: all included or
 13 unsuitable ones excluded. Directions are considered unsuitable for the IFR site when the
 14 dryland area is upwind, and unsuitable for the UUW site when either of two neighbouring
 15 irrigated circles is upwind. See text for specification of the directional sectors.

16

Trace gas	Site	all wind directions		unsuitable directions excluded	
		median flux (nmol m ⁻² s ⁻¹)	N	median flux (nmol m ⁻² s ⁻¹)	N
CH ₄	IFR	25.6	172	26.3	101
CH ₄	UUW	14.0	164	8.73	96
N ₂ O	IFR	0.604	293	0.637	165
N ₂ O	UUW	0.396	279	0.289	131

17

18

1

2 **Table 3.** Estimates of mean annual fluxes, for the period 17 Aug 2012 to 16 Aug 2013, from four approaches: GGR method, NSR method,
 3 mean of the annual means of GGR and NSR, and annual mean of daily values obtained from merging the two methods. Numbers in
 4 parentheses are error estimates from propagation of daily standard errors. N is the number of nights contributing.

5

Trace gas	Site	GGR method		NSR method		GGR and NSR means combined	GGR and NSR merged daily	N
		mean flux (nmol m ⁻² s ⁻¹)	N	mean flux (nmol m ⁻² s ⁻¹)	N	mean flux (nmol m ⁻² s ⁻¹)	mean flux (nmol m ⁻² s ⁻¹)	
CH ₄	IFR	4.7 (0.92)	224	24.3 (1.22)	77	14.5 (0.76)	8.9 (0.79)	259
CH ₄	U UW	6.7 (1.05)	147	12.9 (0.77)	84	9.8 (0.65)	8.9 (0.79)	201
N ₂ O	IFR	0.32 (0.034)	225	0.83 (0.021)	137	0.58 (0.020)	0.47 (0.024)	273
N ₂ O	U UW	0.30 (0.032)	147	0.47 (0.018)	108	0.38 (0.018)	0.36 (0.022)	211

6

7

8

1
2
3
4
5
6
7

8
9
10

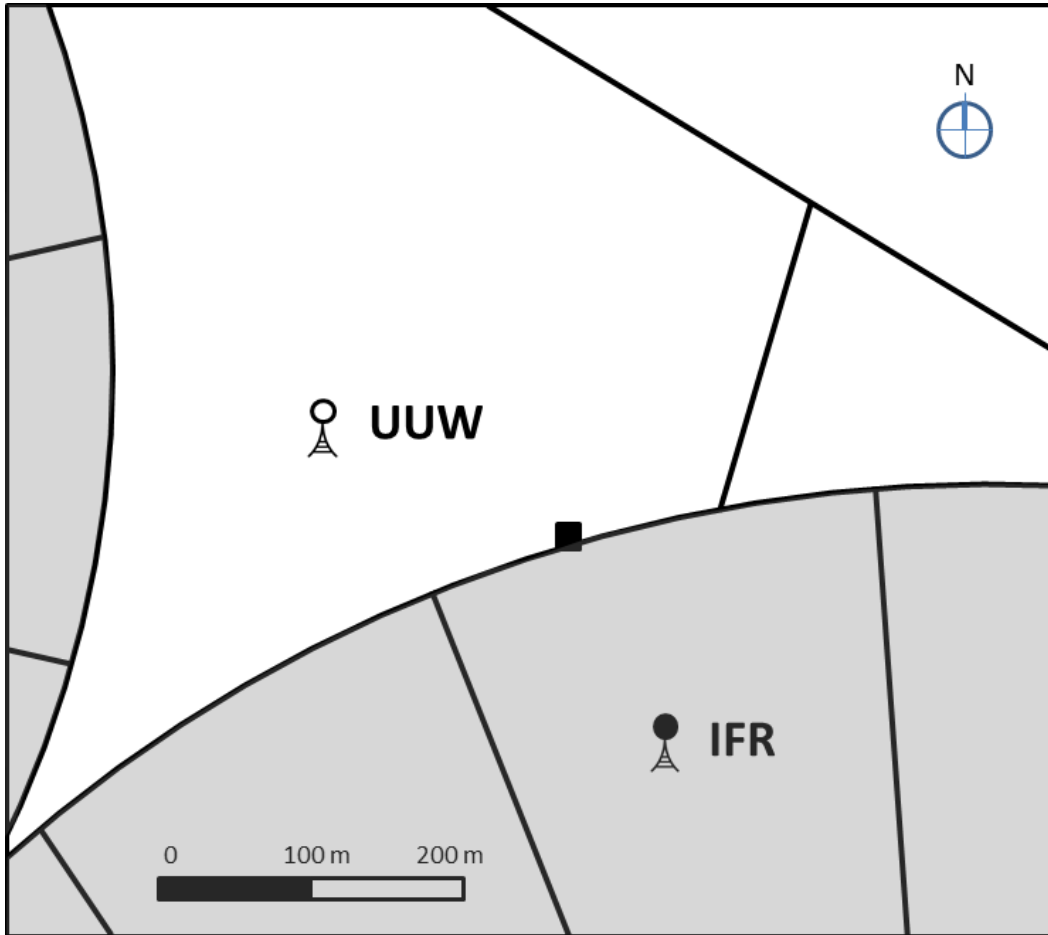
Table 4. Nitrogen budget terms for the IFR site for the year 17 Aug 2012 to 16 Aug 2013. The N₂O emissions value is from the combined GGR and NSR methods, but with a larger uncertainty estimate to account for method discrepancy and potential spatial variability across the irrigated circle. The resulting emission factor is considered a “maximum” because the measured emissions include naturally-occurring background emissions.

Annual N inputs (g N m ⁻²)	
Urea applied	18.3 (1.3)
Excreta (dung, urine, effluent)	23.9 (2.5)
Total	42.2 (2.8)
Annual N ₂ O emissions (g N m ⁻²)	0.51 (0.05)
Maximum emission factor for N ₂ O (%)	1.21 (0.15)

1 **Figures**

2

3



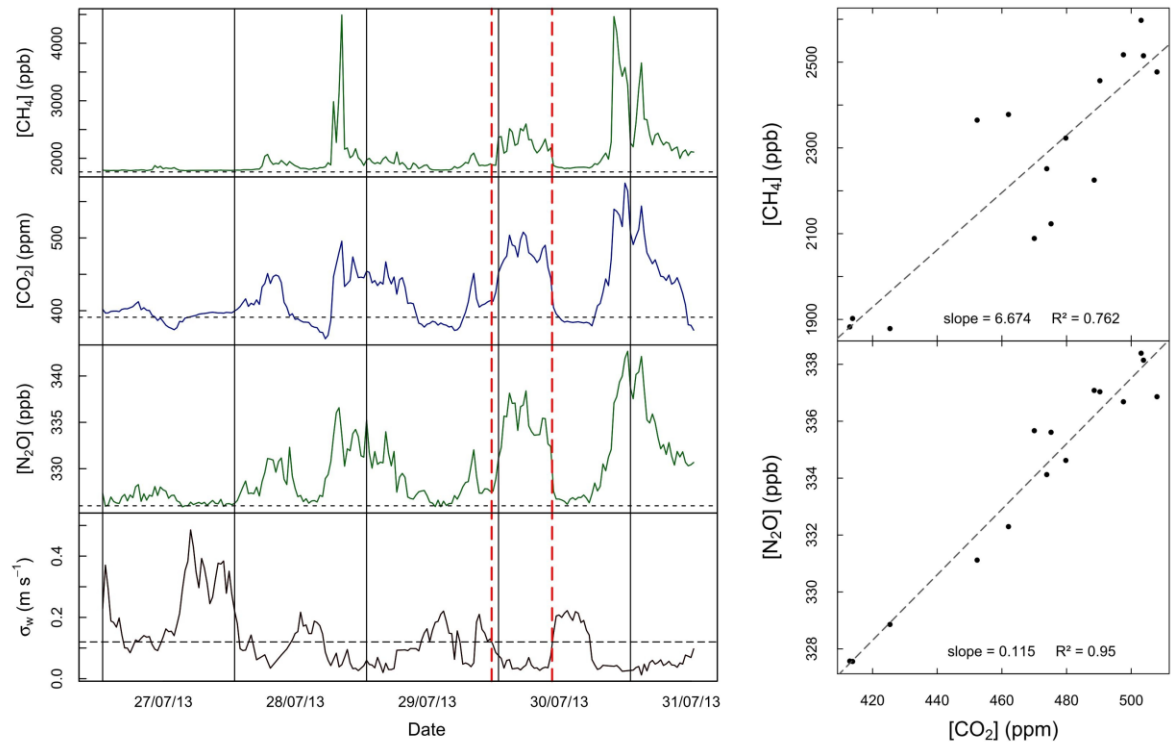
4

5 **Figure 1.** Schematic of the experimental area. The shaded areas represent parts of pivot-
6 irrigated intensively-managed circles of dairy pasture. The white areas are not irrigated. At
7 each of the labelled locations, UUW (unirrigated, unfertilised, winter-grazed) and IFR
8 (irrigated, fertilised, rotationally-grazed), CO₂ fluxes were measured by eddy covariance, and
9 air was sampled from two heights for multi-gas mole-fraction measurements with an FTIR
10 spectrometer. The spectrometer was located in a temperature-controlled hut, indicated with a
11 black square.

12

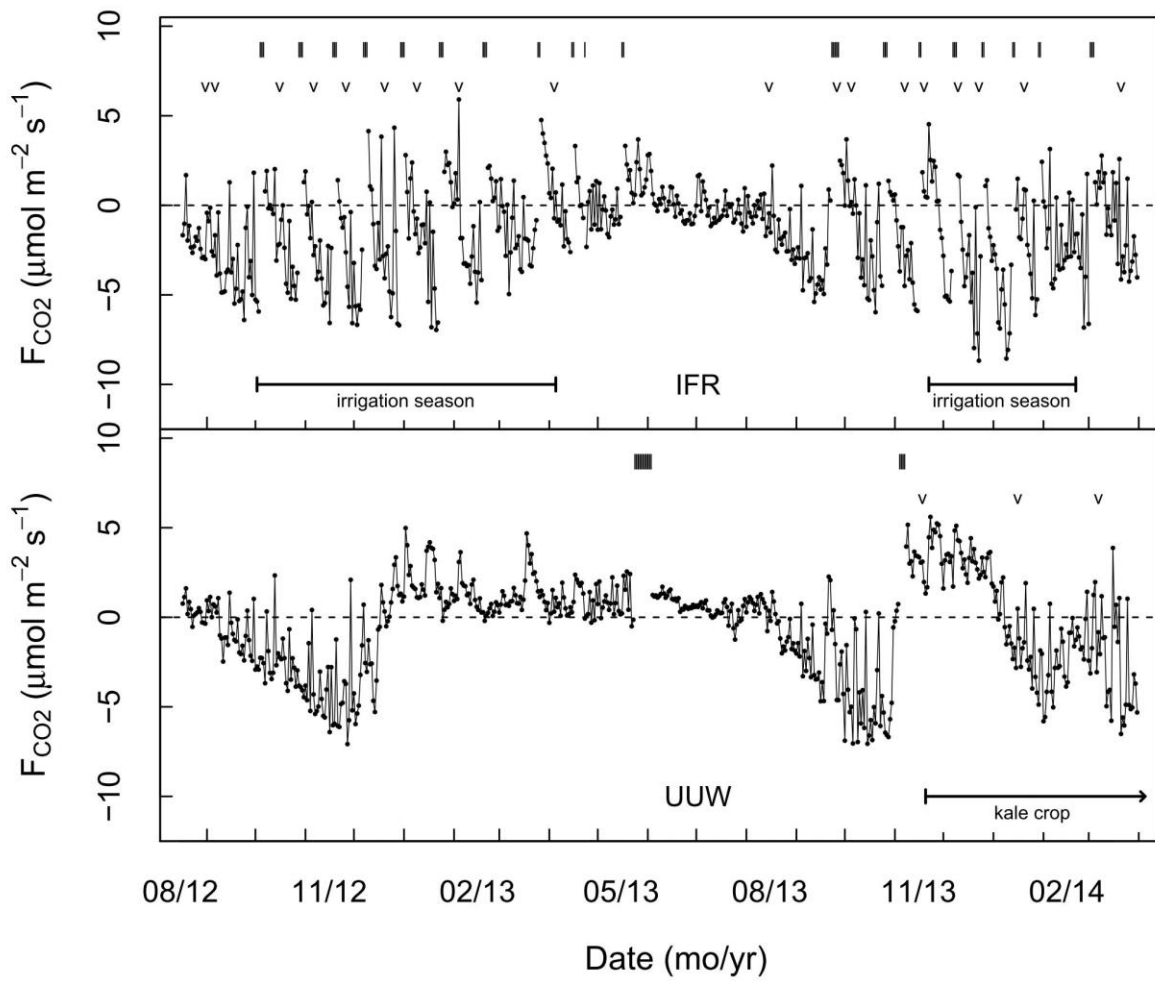
13

14



1
 2 **Figure 2.** Left: evolution of CH₄, CO₂ and N₂O mole fractions (from top to bottom) at 0.76 m
 3 height, as well as standard deviation of vertical wind speed (σ_w), at the IFR site, for a few
 4 days. Horizontal short-dashed lines indicate the southern-hemisphere background values of
 5 the mole fractions. The horizontal long-dashed line marks the low-turbulence threshold for σ_w .
 6 Vertical dashed lines enclose an example period of low turbulence. Right: Linear regressions
 7 of mole fractions for CH₄ (top panel) and N₂O (bottom panel) vs that of CO₂, for this example
 8 period.

9
 10

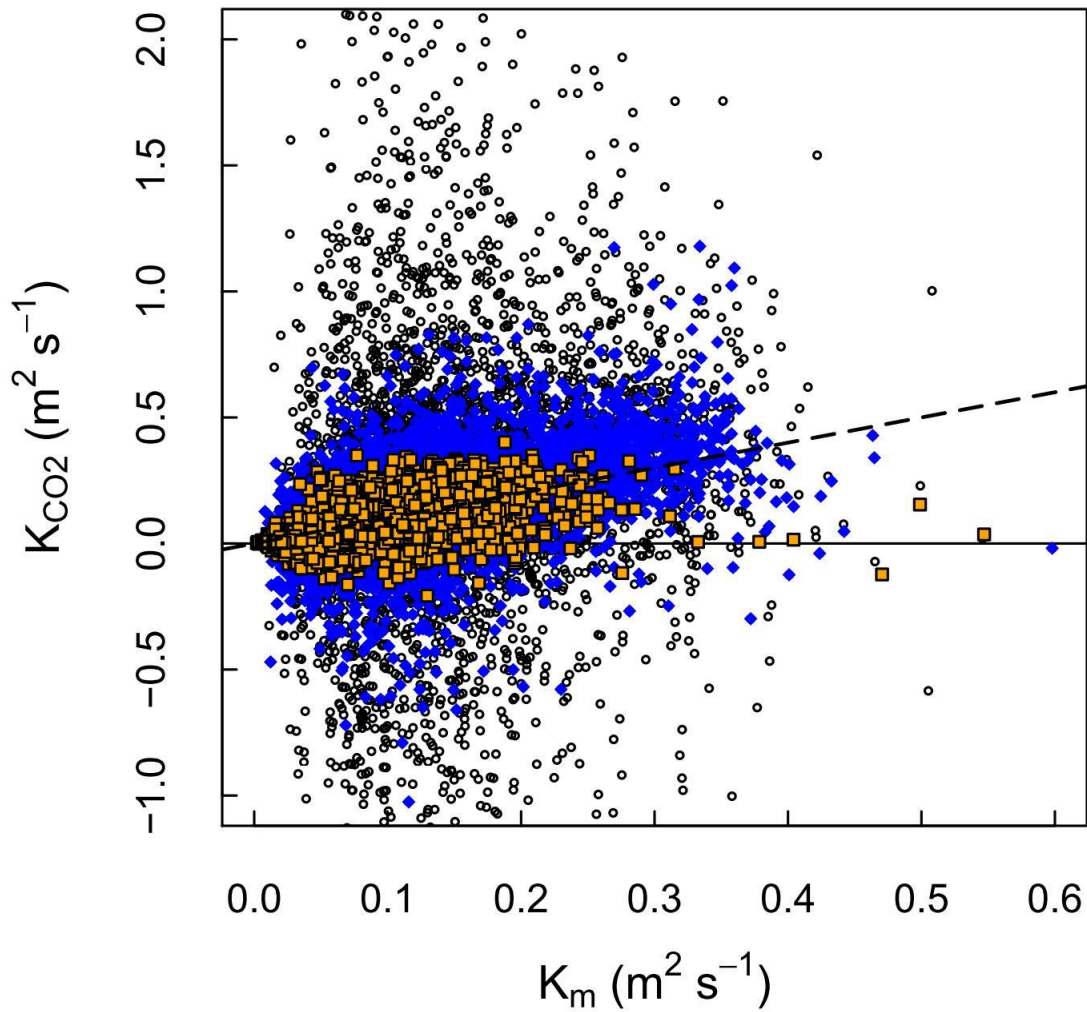


1

2 **Figure 3.** Time series of the daily mean CO₂ flux (net ecosystem exchange) at the IFR site
 3 (top) and the UUW site (bottom). Grazing times are indicated by bars near the top of each
 4 panel. The times of fertiliser applications are marked by “v” symbols.

5

6

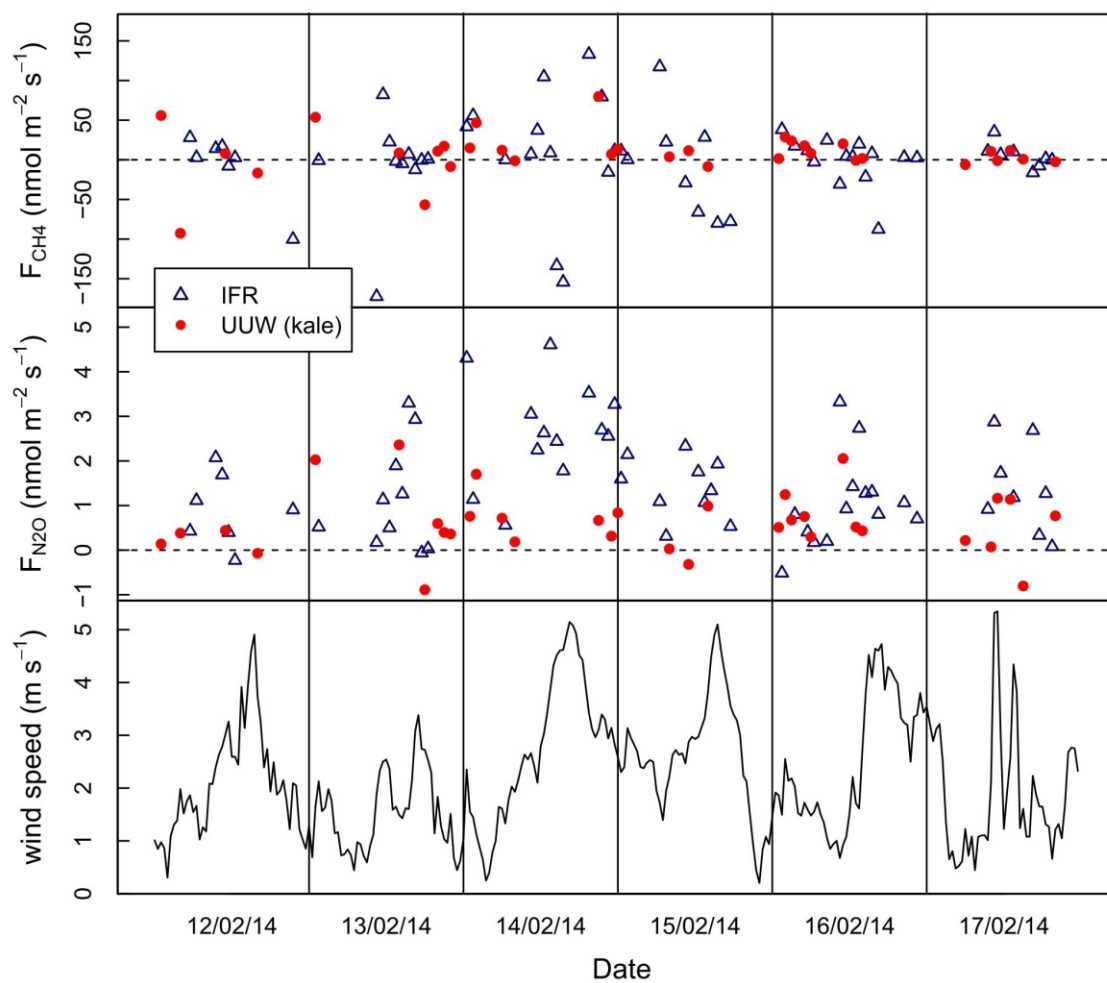


1

2 **Figure 4.** Half-hourly values of the turbulent diffusivity of CO₂ (from gradient measurements
 3 with the FTIR and flux measurements by eddy covariance) versus the diffusivity of
 4 momentum for neutral stratification (from sonic anemometer data), for the IFR site. Open
 5 circles: no filtering of $\Delta[CO_2]$ (mole-fraction difference between intake heights), solid
 6 diamonds: $\Delta[CO_2] < 0.6$ ppm excluded, framed squares: $\Delta[CO_2] < 2.4$ ppm excluded. The
 7 dashed line is the 1:1 line.

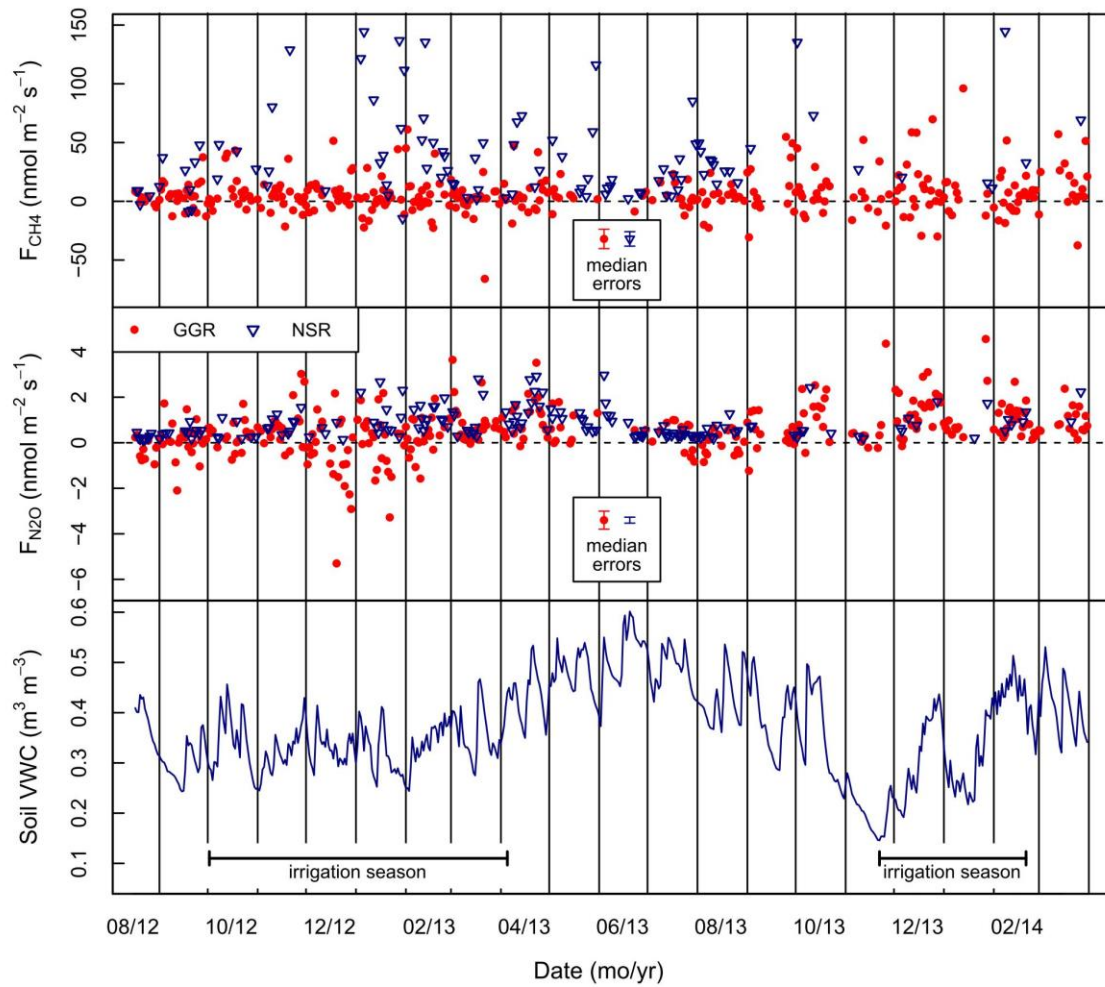
8

9



1
 2 **Figure 5.** Half-hourly fluxes of CH₄ (top) and N₂O (middle) at the two sites, obtained with
 3 the GGR method, as well as wind speed (bottom), for an example period.

4
 5



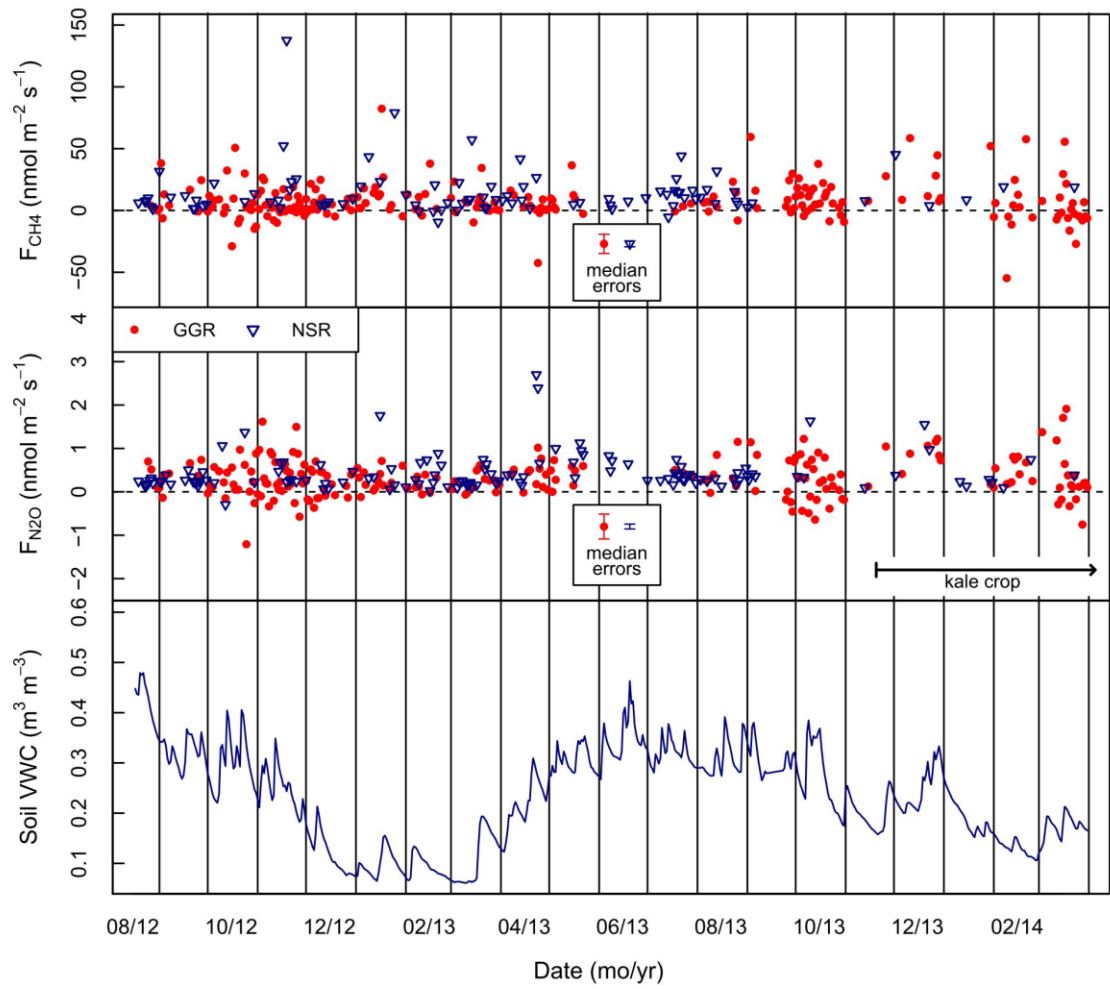
1

2 **Figure 6.** Daily mean fluxes of CH₄ (top) and N₂O (middle) at the IFR site, using the GGR
 3 method (dots) and using the NSR method (triangles). In these two panels, error bars in insets
 4 indicate for each method (GGR left, NSR right) the median of the standard error of the daily
 5 mean flux. Bottom panel: volumetric water content at 5 cm depth.

6

7

8

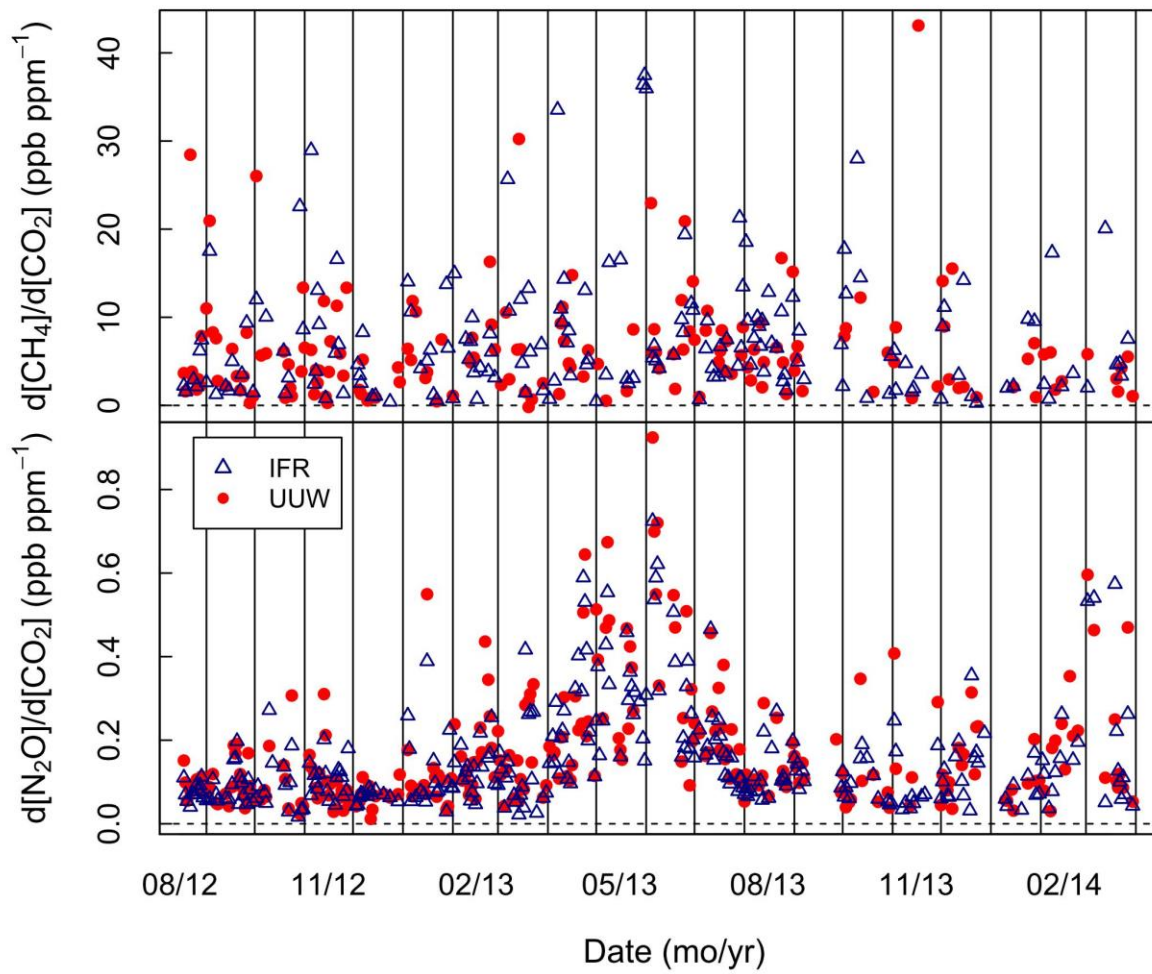


1

2 **Figure 7.** As Figure 6 but for the UUW site.

3

4



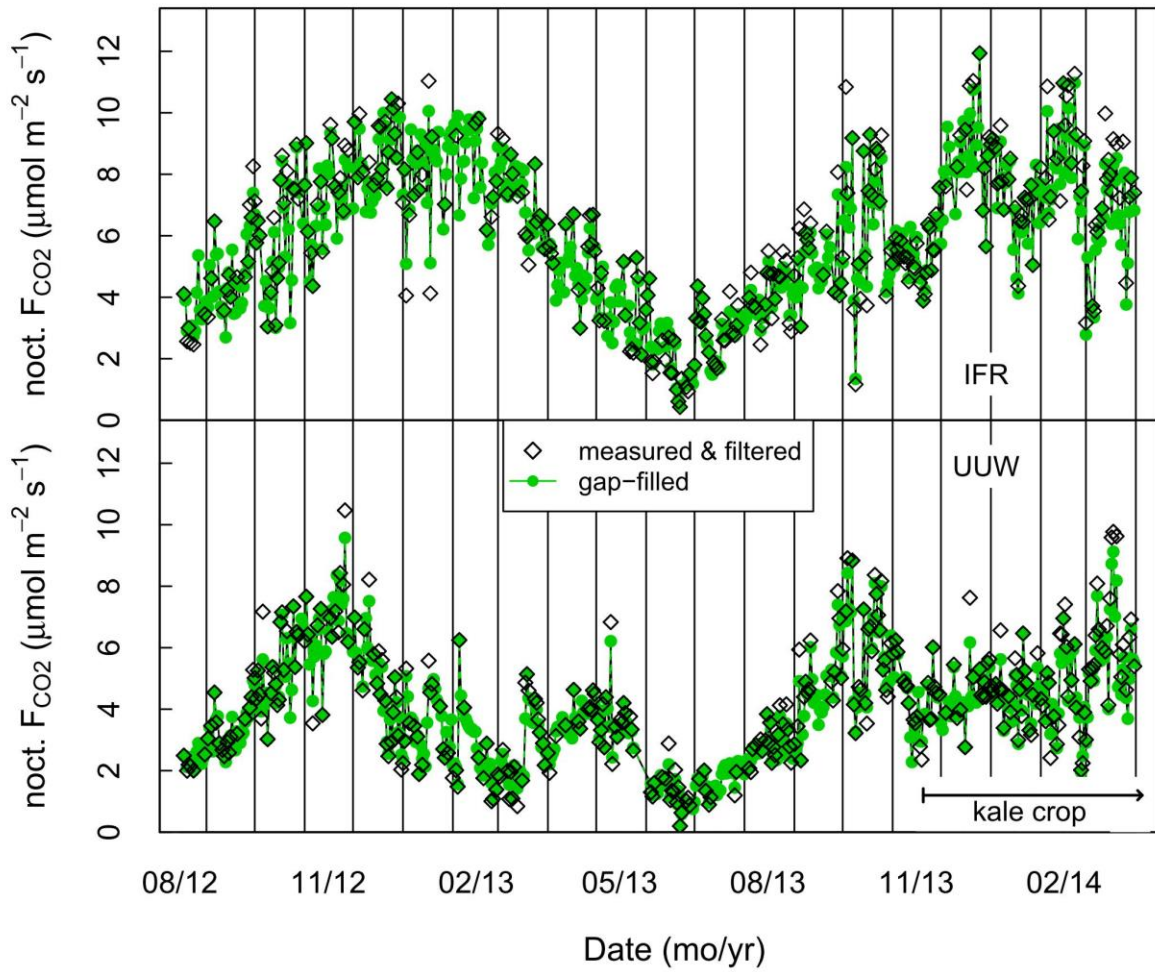
1

2 **Figure 8.** Temporal variation of the slopes of the linear regressions between CH₄ and CO₂
 3 (top panel) and between N₂O and CO₂ (bottom panel), for both sites.

4

5

6



1

2 **Figure 9.** Nocturnal CO₂ emission rates from the IFR site (top) and the UUW site (bottom).
 3 Each point is a whole-night average, obtained either only from measured values during
 4 periods with sufficient turbulence ($\sigma_w > 0.12 \text{ m s}^{-1}$; open diamonds), or from the complete
 5 gap-filled dataset (solid dots).

6

7